SANDIA REPORT
SAND87—1087 • UC—63
Unlimited Release
Printed April 1987

Sizing Handbook for Stand-Alone Photovoltaic/Storage Systems

Richard N. Chapman

Prepared by
Sandia National Laboratories
Albuquerque, New Mexico 87185 and Livermore, California 94550
for the United States Department of Energy
under Contract DE-AC04-76DP00789

When printing a copy of any digitized SAND Report, you are required to update the markings to current standards.

SF2900Q(8-81)

Issued by Sandia National Laboratories, operated for the United States Department of Energy by Sandia Corporation.

NOTICE: This report was prepared as an account of work sponsored by an agency of the United States Government. Neither the United States Government nor any agency thereof, nor any of their employees, nor any of their contractors, subcontractors, or their employees, makes any warranty, express or implied, or assumes any legal liability or responsibility for the accuracy, completeness, or usefulness of any information, apparatus, product, or process disclosed, or represents that its use would not infringe privately owned rights. Reference herein to any specific commercial product, process, or service by trade name, trademark, manufacturer, or otherwise, does not necessarily constitute or imply its endorsement, recommendation, or favoring by the United States Government, any agency thereof or any of their contractors or subcontractors. The views and opinions expressed herein do not necessarily state or reflect those of the United States Government, any agency thereof or any of their contractors or subcontractors.

Printed in the United States of America
Available from
National Technical Information Service
U.S. Department of Commerce
5285 Port Royal Road
Springfield, VA 22161

NTIS price codes
Printed copy: A03
Microfiche copy: A01

SAND87–1087
Unlimited Release
Printed April 1987

Distribution
Category UC–63

Sizing Handbook for Stand-Alone Photovoltaic/Storage Systems

Richard N. Chapman
Division 6223
Sandia National Laboratories
Albuquerque, NM 87185

Abstract

This report details the use and development of a simplified sizing technique for stand-alone photovoltaic/storage systems. The array size and storage capacity are chosen to achieve the required loss-of-load probability (LOLP). The LOLP represents the level of confidence at which the system will satisfy the load. An LOLP of 0 means that the load will always be satisfied, and an LOLP of 1 means that the load will never be satisfied. Array sizes are read from array-sizing nomograms as a function of latitude, tilt angle, and average horizontal insolation in December (in the northern hemisphere) or June (in the southern hemisphere). Storage capacities are read from storage-sizing nomograms as a function of the required LOLP. The technique is valid for systems with a fixed tilt array, product or energy storage, and for any hourly load profile or daily load profile within a given month. The only constraint is that the average monthly load must not vary more than ± 10% from month to month. The designer can choose from tilt angles from latitude minus 20° to latitude plus 20° and can choose from a range of array size/storage capacity combinations for any given LOLP.

INTRODUCTION

A stand-alone photovoltaic/storage system can be defined as a power source dedicated to some load such as a water pump, refrigerator, or radio transmitter. The phrase "stand-alone" implies that the photovoltaic/storage system is the only source from which the load may draw power. The power generated by the photovoltaic (PV) array is equal to the insolation incident on the plane of the array's surface (plane-of-array insolation, POA) multiplied by the array's area and efficiency. The power generated by the array varies not only with the daily and seasonal cycles of the sun, but also with changing weather conditions. Because the power required by the load does not usually track the magnitude of the insolation, a portion of the energy produced by the array must be stored to be able to satisfy the load when there is insufficient insolation. The system designer must somehow quantify the variability in the insolation and from that choose a combination of array size and storage capacity that will satisfy the load at the confidence level required by the user.

This confidence level is mathematically described by the loss-of-load probability (LOLP), which represents how often the PV/storage system will not be able to satisfy the load. An LOLP of 0 means that the load will always be satisfied, and an LOLP of 1 means that the load will never be satisfied. The LOLP is characterized by an average or long-term value and the distribution about that average value. For conventional power sources, like a diesel generator, the distribution about the long-term value is narrow and smooth. For PV/storage systems, the distribution can be wide and erratic. The importance of this type of distribution is that if the variability in the insolation is not accurately quantified, the system may be over- or undersized.

A PV/storage system fails to satisfy the load when the power generated by the array is insufficient and the storage is depleted. Energy is stored when the power generated by the array is greater than the load. Energy is taken from storage when the power generated by the array is less than the load. The amount of stored energy at any given time depends on the sequence of instantaneous insolation and load levels from the last time that the storage was either depleted or at full capacity. An infinite number of sequences can lead to depletion of storage. Consequently, continuous insolation and demand profiles for the expected life of the system are required to determine the long-term LOLP and its distribution.

Because we cannot predict the weather, we are forced to rely on long-term historical data to define the insolation profile. There are long-term records of hourly direct normal and horizontal insolations from which the POA insolation can be calculated. These data, however, are available for only a handful of sites worldwide. Even if these data are available, their direct use requires extensive computer support, which is both expensive and time-consuming.

The demand profile is a function of the application and can have many forms. For example, a telecommunication system would have a nearly constant demand profile. An irrigation system would have a well-defined seasonal profile. A vaccine refrigerator system might have a highly erratic, unpredictable profile. In fact, the demand profile for most stand-alone applications is not well defined. We

will show that short-term variations in the demand have little effect on the long-term LOLP and that monthly average values of the demand are adequate for defining the load profile. Furthermore, if the monthly average demands do not vary by more than ± 10%, the average yearly demand is adequate. This sizing handbook describes an accurate noncomputerized sizing technique that allows the designer to size for the required LOLP given the average yearly demand and readily available insolation data.

The technique was derived using a loss-of-load simulation model and 23.5 years of hourly insolation data from the 20 U. S. weather stations listed in Table 1. These data were obtained from the SOLMET data base (1), which is a compilation of hourly solar and meteorological observations. Correlations were derived that relate the variability in the POA insolation to the average December horizontal insolation (in the northern hemisphere) or the average June horizontal insolation (in the southern hemisphere). These correlations were then used to generate sizing nomograms that give the storage capacity as a function of the loss-of-load-probability (LOLP), and the array size as a function of the array tilt angle, the average horizontal insolation, and latitude of the site.

Table 1. Solmet Sites Used to Develop Sizing Technique.

Albuquerque, New Mexico	Medford, Oregon
Miami, Florida	Nashville, Tennesse
Apalachicola, Florida	New York, New York
Dodge City, Kansas	Phoenix, Arizona
Brownsville, Texas	Ely, Nevada
Cape Hatteras, North Carolina	Charleston, South Carolina
Lake Charles, Louisiana	Caribou, Maine
Great Falls, Montana	Seattle, Washington
Bismarck, North Dakota	Fresno, California
Madison, Wisconsin	Columbia, Missouri

The sizing nomograms give the array size in terms of design insolations and the storage capacity in terms of days of storage. The design insolation and days of storage are translated into the array area and storage capacity based on the magnitude of the demand, the system configuration, and the performance characteristics of the system components.

Four sets of array and storage-sizing nomograms were derived that define a curve of array size versus storage capacity from which the designer can choose equivalent array/storage size combinations ranging from small array/large storage capacity to large array/small storage capacity. The array/storage combinations are equivalent in that all result in the same LOLP. Each set of sizing nomograms contains five array-sizing nomograms, one each for tilt angles of latitude minus 20 and 10°, latitude, latitude plus 10 and 20°, and one storage-sizing nomogram.

The 20 sites represent most climates found worldwide. The fact that these correlations were derived from data representing such a wide range of climates indicates that the variability in insolation

does not depend on the climate. The work of Liu and Jordan (2) and Klein (3) support this observation.

Liu and Jordan noted that the distribution of daily horizontal insolations for a given month is dependent only on the average monthly clearness index and not on the type of climate. Klein has shown that persistence of weather, that is the dependence of today's insolation on yesterday's insolation, is weak and fairly constant from site to site regardless of the climate. The implication of these observations is that there is no correlation between climate and variability in insolation. Because this technique is based on the variability in the insolation and not on the magnitude of the insolation, it can be applied to sites outside the U. S. even if the climate is not represented by one of the 20 sites.

The technique is applicable to any system with a fixed tilt array. The sizing nomograms are valid for any hourly demand profile or daily demand profile within a given month and for any type of storage (i.e., energy or product storage). The only limitation of this technique is that the average monthly demand must not vary by more than ± 10%. We recently developed sizing nomograms that are based on monthly values of the long-term LOLP and can be used for applications in which the average monthly demand varies by more than ± 10%.

The sizing technique is presented in the next section and is followed by detailed sizing examples for general power load and direct coupled water pumping applications. The sizing nomograms can be found in Appendices A1 through A4. The derivation of the loss-of-load simulation model is given in Appendix B along with model verification and an overview of how the technique was developed.

SIZING PROCEDURE

This section describes the four steps in applying the sizing technique. (Detailed sizing examples are given in the following section.) The first step involves defining site- and application-specific parameters. The second and third steps involve using the sizing nomograms found in Appendices A1, A2, A3, and A4 to determine the required array size and storage capacity. This technique gives the designer four sets of array size/storage capacity combinations. These combinations define a curve-of-array size versus storage capacity that satisfies the required LOLP defined in step one. The sizes vary from large array area/small storage capacity to small array area/large storage capacity.

After performing these three steps, the designer will have array sizes in terms of design insolations and storage capacities in terms of days of storage. The translation of the design insolations and days of storage into array size/storage capacity combinations is the next step in the design sequence. The procedure for this step depends on the system's configuration and it cannot be generalized. A comprehensive discussion of this phase of design is beyond the scope of this document. We do, however, present specific examples of this design effort in step four of the sizing procedure.

Step One. Define Site- and Application-Specific Parameters

The following sections define the site and application parameters and give guidelines on how they are specified.

Site-specific parameters - These parameters consist of the latitude and the average horizontal insolation in December (in the northern hemisphere) or June (in the southern hemisphere). (Some readers who are more familiar with calculations of insolation incident of flat surfaces may wonder why the ground reflectance is not included as a site-specific parameter. The degree of uncertainty inherent in insolation data and this sizing technique do not warrant such detail in the description of the site. We found that the ground reflectance could be preset at an average value without reducing accuracy.)

Monthly average horizontal insolations have been tabulated for many sites worldwide (4,5). If a tabulated value for the horizontal insolation cannot be found for the particular region, an estimate can be obtained from worldwide insolation maps (5,6).

Application-specific parameters - These parameters include the daily energy demand and the desired LOLP. The sizing nomograms were derived assuming a "constant" demand. Figure 1 shows, however, that the hourly demand has very little effect on the sizing nomograms. Figure 1 was generated by deriving the four storage-sizing nomograms for hourly demand profiles ranging from

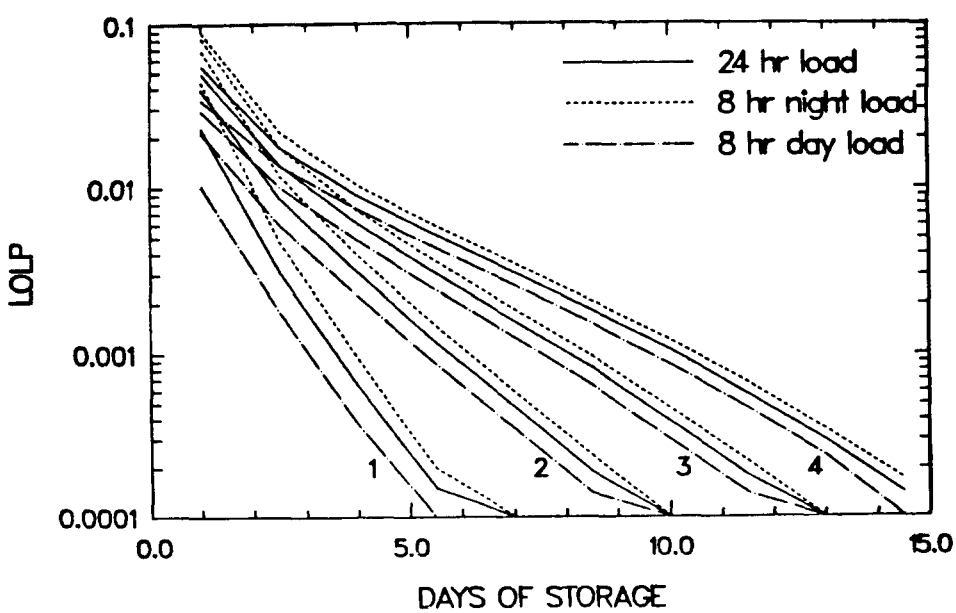

Figure 1. Effect of hourly demand profile on storage-sizing nomogram.

an 8-hour nighttime demand to an 8-hour daytime demand without altering the array-sizing nomograms. It shows that the array size and storage capacity required for a given LOLP are nearly independent of the hourly demand profile. The technique is valid for any hourly demand profile.

Figure 2 shows that the daily demand profile within a given month has little effect on the sizing nomograms. Figure 2 was generated by randomly varying the total daily demand within each month as shown in Figure 3. The daily demand values range from 0 to 200% of the average daily demand and have a standard deviation of approximately 40%. The technique is also valid for any daily demand profile within a given month provided that the average daily demand does not vary by more than ± 10% from month to month.

(A more difficult issue is how to deal with seasonally varying demands, especially summer peaking demands. We have recently developed sizing nomograms that are based on long-term monthly LOLP values and can be used to size systems with seasonally dependent loads. The use of these nomograms is essentially the same as the use of the nomograms presented in this report. The difference is that these recent nomograms are used to size a system that will achieve the required LOLP in a given month as opposed to a system that will achieve the required overall LOLP. As a result, the designer must size a system for each month, determine which system size satisfies the monthly LOLP criterion for all months, and then calculate the overall LOLP. These monthly sizing nomograms will be published in a separate document.)

The LOLP represents the fraction of the demand that will probably not be satisfied over the life of the PV/storage system. This long-term LOLP is the summation of 20 plus yearly LOLPs. Unlike conventional energy sources that have a narrow distribution of yearly LOLPs about the long-term LOLP, photovoltaic energy sources have a very wide distribution of yearly LOLPs as shown in Figure 4. This type of distribution is to be expected given the nature of solar energy sources: their performance changes as the weather changes. This characteristic of PV/storage systems must be considered when a long-term LOLP is chosen, because even if the long-term LOLP is very low, there can still be years with relatively high LOLPs. To eliminate all periods of high LOLP, the designer would have to oversize a PV/storage system to the point that it would probably not be cost-effective or practical. If no periods of high LOLP can be tolerated, a PV/storage/diesel hybrid system should be considered.

Step Two. Determine Four Sets of Array Sizes in terms of Design Insolations

The design insolation (POA_0) is read as a function of the latitude, the tilt angle of the array, and the average horizontal design month insolation from array-sizing nomograms found in Appendices A1 - A4. Each of these appendices contains one set of array size and storage capacity nomograms. The design insolation

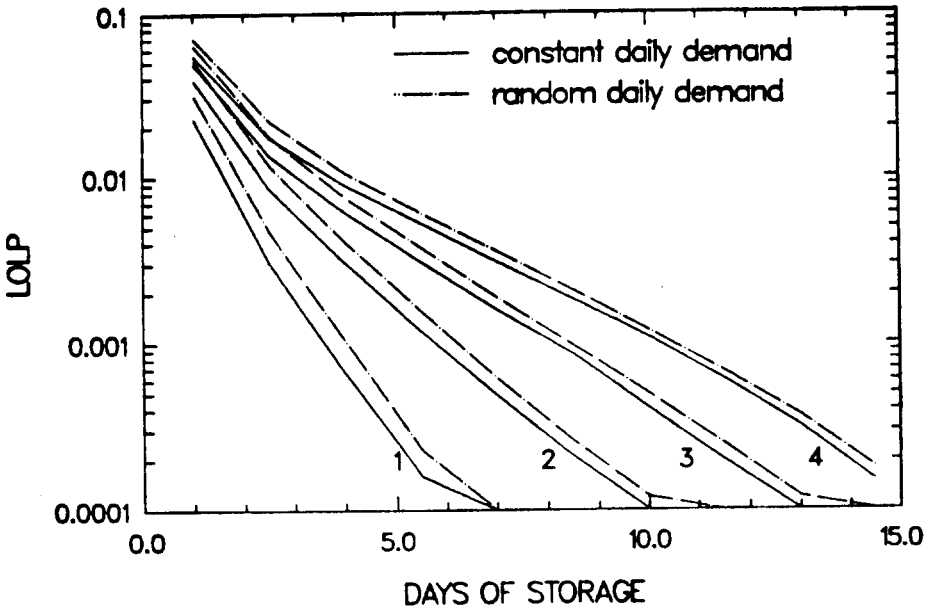

Figure 2. Effect of daily demand profile on storage-sizing nomograms.

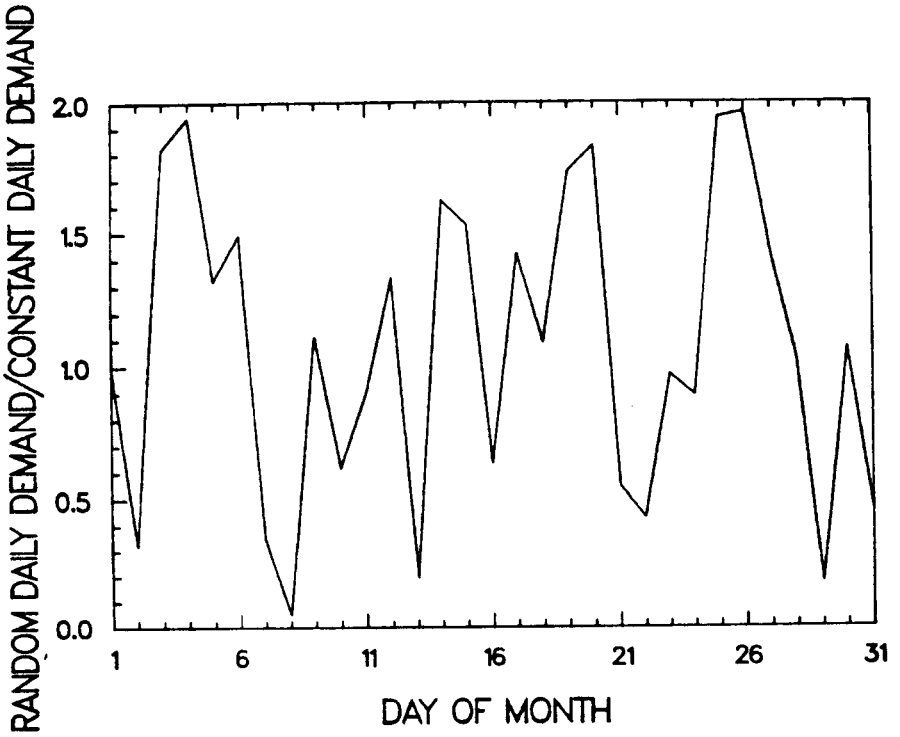

Figure 3. Example of random daily demand profile within a 31-day month.

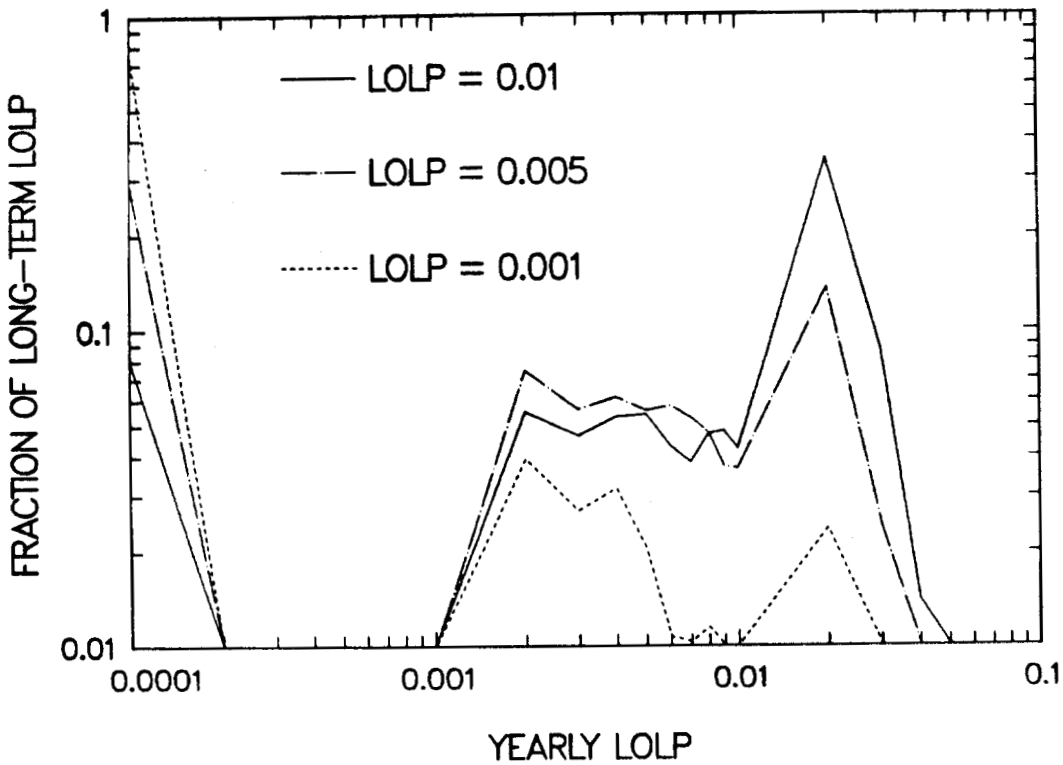

Figure 4. Distribution of yearly LOLPs for various long-term LOLPs.

is a strong function of the tilt angle. This dependency is handled by providing a series of array-sizing nomograms, one each for tilt angles of latitude minus 20 and 10°, latitude, and latitude plus 10 and 20°, in each set of sizing nomograms. At some point in the design process, the designer must select a tilt angle. He must then use the POA_0 values corresponding to that tilt angle for sizing the array. The minimum theoretical array size is achieved by selecting the tilt angle that gives the largest value of POA_0. In practice, however, this tilt angle may not be the best choice. For example, if the ground is normally snow covered during the winter, it may be best to tilt the array at a larger angle to help keep the array surface free of snow.

Step Three. Determine Four Storage Capacities in terms of Days of Storage

The days of storage required (S) are a function of the long-term LOLP and are read off the storage capacity nomograms found in Appendices A1 - A4. The storage capacity required to achieve a given LOLP is not a function of the tilt angle. Therefore, each set of sizing nomograms contains a single storage-sizing nomogram. At the end of step 3, the designer has four sets of design insolations (POA_0)/days of storage (S) combinations, all for the chosen LOLP (see Tables 2 and 5). Each set consists of one S value and five POA_0 values. Each POA_0 value corresponds to one of the five tilt angle options.

Step Four. Determine Array Area and Storage Capacity

The objective of this step is to specify an array area and storage capacity for the components chosen by the designer. To do this, the designer must define two parameters; the insolation to storage path efficiency (η_{in}) and the storage to demand path efficiency (η_{out}).

The path efficiencies are the product of the efficiencies of the components that comprise the energy flow streams from insolation to storage and storage to demand. For example, examine the schematic shown in Figure 5. The components in the insolation to storage path are the array, the maximum power tracker, the charge controller, and the batteries. The components in the storage to demand path are the batteries, the charge controller, and the inverter.

The correct values for the path efficiencies are the average daily efficiencies in the design month defined as

$$\eta_{in} = \frac{\text{daily POA A}}{\text{daily energy added to storage}} \tag{1}$$

$$\eta_{out} = \frac{\text{daily energy taken from storage}}{\text{demand}}, \tag{2}$$

where daily POA is the total average insolation in the design month, A is the array area, and demand is the average total daily demand.

The determination of the path efficiencies is complicated when the instantaneous component efficiencies are interrelated. In such cases, it is necessary to perform a single-day hourly simulation representing an average day in the design month.

The relationship between the array area, the path efficiencies, the daily demand, and the design insolation is defined as

$$\text{demand}/\eta_{out} = \text{POA}_0 \text{ A } \eta_{in}. \tag{3}$$

The relationship between the storage capacity (CAP), the days of storage (S), the path efficiencies, and the total daily demand is defined as

$$\text{CAP} = (\text{S demand})/\eta_{out}. \tag{4}$$

Assume that we are sizing the system shown in Figure 5 and that the average daily efficiencies of the components are

array	- 0.10
maximum power tracker	- 0.95
charge controller	- 0.95
battery charge	- 0.75
battery discharge	- 1.00
inverter	- 0.85.

For these components, η_{in} is (0.10)(0.95)(0.95)(0.75) or 0.068 and η_{out} is (1.00)(0.85) or 0.85. If the daily demand is

10 kWh/day and POA_0 is 5 kWh/m^2-day, the array area is (10)/(5)(0.068)(0.85) or 35 m^2. If the value for S is 3, the required storage capacity is (3)(10)/(0.85) or 35 kWh. If the maximum allowable depth of discharge for the battery is 0.8, the required battery rating is (35)/(0.8) or 44 kWh.

It is important to re-emphasize that this techniques gives the designer a curve of array size versus storage capacity from which the designer can choose array/storage size combinations that satisfy the LOLP. An economic analysis should be performed to determine which system is the most cost effective. Keep in mind, however, that there may be other criteria that have a higher priority than costs. For example, the system might power a concealed security sensor, in which case a minimally exposed array would have a high priority. (We do intend to develop an economics handbook for stand-alone systems, which will be published as a separate document.)

SIZING EXAMPLES

This section steps the reader through specific applications of the sizing technique for a general load electrification system with battery storage and a direct coupled water pumping system with water storage. Sizing worksheets are provided to help organize and clarify the sizing procedure. Table 2 shows a completed worksheet for the electrification system and Table 5 shows a completed worksheet for the water pumping system.

Table 2. Completed worksheet for electrification system.

SIZING WORKSHEET

Latitude	30 N	
Design month	December	
Average horizontal insolation in design month	3.0	(kWh/m^2-day)
Loss-of-load probability	0.001	

Design insolations and days of storage

Size Set	Design Insolation, POA_0 (kWh/m^2-day) tilt angle, latitude plus -20	-10	0	10	20	Days of Storage, S
1	3.00	3.23	3.37	3.44	3.45	3.59
2	3.53	3.93	4.28	4.50	4.46	5.80
3	3.73	4.21	4.61	4.84	4.71	8.13
4	3.85	4.38	4.79	4.99	4.79	10.19

Electrification

Step One.

Assume that the system is at latitude 30° north, the average horizontal insolation in December is 3 kWh/m^2-day, and that the daily demand is 5 kWh ac. Assume that the electrical load is primarily vaccine refrigeration. For this critical load we will require an LOLP of 0.001.

Step Two.

The design insolation values listed in the worksheet for this system (Table 2) were read from Figures A1a-e, A2a-e, A3a-e, and A4a-e for a latitude of 30° north and a horizontal insolation of 3 kWh/m^2-day. We will select the tilt angle that gives the largest POA_0 values. For this example, that tilt angle is latitude plus 10°.

Step Three.

The days of storage values listed in Table 2 were read from Figures A1f, A2f, A3f, and A4f for an LOLP of 0.001.

Step Four.

Figure 5 shows the schematic for this electrification system. The components in the insolation to storage path are the array, a maximum power tracker, a battery charge controller, and the batteries. The components in the storage to demand path are the batteries and an inverter.

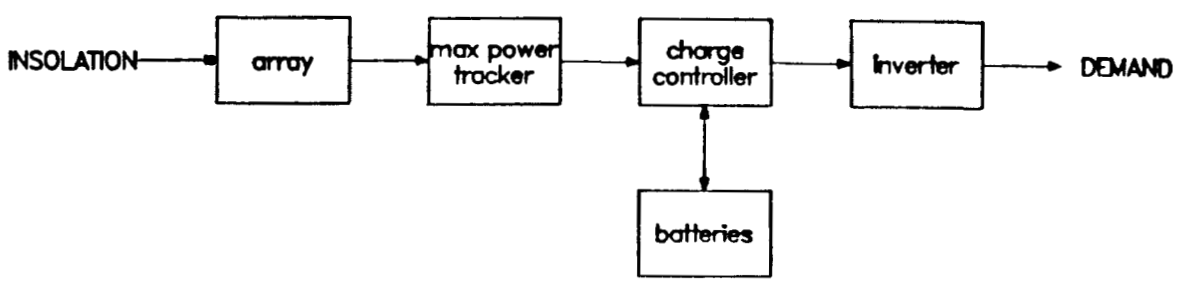

Figure 5. Schematic for electrification system.

The operating voltage in this system is regulated. The component efficiencies are not interrelated and can be evaluated independently. Therefore, it is not necessary to perform a single-day simulation. Once the designer selects the components and specifies their performance, he can translate the design insolation and days of storage values directly into array configurations and storage capacities.

Component specifications

The inverter rating is matched to the anticipated peak demand. For this example, we will assume the demand profile given in Table 3, which shows that the peak demand is 1000 Wac. We will select a

1200 Wac/12 Vdc inverter. The inverter's efficiency is a function of its load factor, which is the ratio of the actual demand to its rating. Table 3 shows the hourly values for the load factor and efficiency along with the resulting daily efficiency.

Table 3. Hourly values for demand, inverter load factor, and inverter efficiency.

hour	demand (Wac)	load factor	efficiency	dc input (Wdc)
15	200	.167	.40	500
16	600	.500	.84	714
17	1000	.833	.90	1111
18	1000	.833	.90	1111
19	800	.667	.88	909
20	600	.500	.84	714
21	400	.333	.75	533
22	200	.167	.40	500
23	200	.167	.40	500
totals	5000			6592

average daily efficiency = 5000/6592 = 0.758

The performance of batteries is extremely complicated and cannot be predicted -- especially when subjected to the uncontrolled charge/discharge cycles that occur in stand-alone photovoltaic systems. Furthermore, it is difficult to measure separate charge and discharge efficiencies of batteries. Consequently, battery efficiencies are usually given in terms of a constant round-trip efficiency. The choice of battery depends on the environment of the site, how often the battery can be serviced, and on how the battery is cycled. (The economics handbook will contain information on how the battery is cycled as a function of the required LOLP and the days of storage.) Given this information, a battery manufacturer can suggest an appropriate battery. For this example, we will select a 12 Vdc deep-discharge battery with a maximum depth-of-discharge of 0.8 and a round-trip efficiency of 0.75.

The battery capacity is usually defined in terms of the amount of energy that can be extracted, not the amount of energy that is actually stored. To be consistent with these conventions, the battery charge efficiency is set equal to the round trip efficiency and the battery discharge efficiency is set equal to 1.

The maximum power tracker adjusts the array voltage to the maximum power point. The array efficiency at the maximum power point (η_{mp}) is a function of the cell temperature (T_c) and the array's efficiency at some reference temperature (η_r, T_r) and is given by

$$\eta_{mp} = \eta_r \, [1. - C_T(T_c - T_r)], \qquad (5)$$

where C_T is the maximum power temperature coefficient. We will

select a 0.36 m^2 module with an efficiency of 0.10 at 48°C and a temperature coefficient of 0.005/°C. In general, the average daily array temperature is from 5 to 15 °C above the average daylight ambient temperature. We will assume that the the average ambient daylight temperature in the design month at this site is 10°C and that the average array temperature is 20°C, which results in an average daily array efficiency of 0.114. The maximum error introduced by this assumption is about 2%. The maximum power voltage of the module is 16.5 V and the maximum power current is 2.45 A.

Both the maximum power tracker and the battery charge controller have small parasitic power draws. We will assume that both have constant efficiencies of 0.95.

Select array configuration/storage capacity configurations

The insolation to storage path efficiency (η_{in}) is the product of the array, maximum power tracker, battery charge controller, and the battery round trip average daily efficiencies and is equal to 0.077. The storage to demand path efficiency (η_{out}) is the product of the charge controller and the inverter efficiencies which is 0.720. Using equation (3) and the four POA_0 values (tilt angle of latitude plus 10°) obtained from the array-sizing nomograms, we find that applicable array areas range from 17.2 m^2, corresponding to 48 modules, to 24.9 m^2, corresponding to 69 modules. Since the nominal battery and inverter voltage is 12 V, the modules would be grouped in parallel.

The storage capacities are calculated using equation (4), the days of storage, and η_{out}. Because the maximum depth-of-discharge for the selected battery is 0.8, the storage capacities are increased by (1)/(0.8). Table 4 lists several array configuration/storage capacity combinations that will satisfy an LOLP of 0.001. The days of storage corresponding to each array configuration were determined by interpolating between the four POA_0 values.

Table 4. Applicable array configurations/storage capacities for electrification system.

# modules	A (m^2)	POA_0 (kWh/m^2-day)	S	Capacity (kWh)
48	17.3	4.96	9.78	84.9
53	19.1	4.49	5.78	50.2
57	20.5	4.18	5.13	44.5
61	22.0	3.90	4.55	39.5
65	23.4	3.66	4.05	35.2
69	24.8	3.45	3.61	31.3

Water Pumping

Step One.

For this example, we will assume that the site latitude is 10° south, the average horizontal insolation in June is 4 kWh/m^2-day, and that the daily water demand is 10 m^3. Assume that the demand

is primarily for potable water and that an LOLP of 0.01 is acceptable.

The power required to pump water is the mass flow rate multiplied by the total dynamic head (H). Assume that the total dynamic head for this application is 5 m. The density of water is 1000 kg/m^3. The mass flow rate is the volume of water pumped (V) multiplied by the density (ρ) divided by the time (t) during which the water was pumped. Since the total energy requirement (E) is the power multiplied by the time, we have

$$E = V \rho H. \tag{6}$$

The daily demand for this application is then (10)(1000)(5) = 75,000 kg-m/day or 0.204 kWh/day.

Step Two.

The design insolation values read from the array-sizing nomograms (Figures A1a-e, A2a-e, A2a-e, and A4a-e) are shown on the worksheet (Table 5). The values correspond to latitude 10° south and a horizontal June insolation of 4 kWh/m^2-day. We will select the tilt angle that gives the largest POA_0 values. For this example, that tilt angle is latitude plus 10°.

Step Three.

The values of days of storage listed on the worksheet (Table 5) were read from the storage-sizing nomograms (Figures A1f - A4f). These values correspond to an LOLP of 0.01.

Table 5. Completed sizing worksheet for direct coupled water pumping system.

SIZING WORKSHEET

Latitude	10 S	
Design month	June	
Average horizontal insolation in design month	4.0	(kWh/m^2-day)
Loss-of-load probability	0.01	

Design insolations and days of storage

Size Set	Design Insolation, POA_0 (kWh/m^2-day) tilt angle, latitude plus -20	-10	0	10	20	Days of Storage, S
1	3.03	3.10	3.13	3.13	3.10	1.61
2	3.55	3.81	4.07	4.22	4.14	2.35
3	3.74	4.10	4.42	4.58	4.42	3.08
4	3.87	4.28	4.61	4.74	4.52	3.74

Step Four.

Figure 6 is a schematic for this direct coupled water pumping system with water storage. The components in the insolation to storage path are the array and the motor/pump set. Since the water distribution is gravity fed, there are no components in the storage to demand path. The storage to demand path's efficiency (η_{out}) is therefore 1.

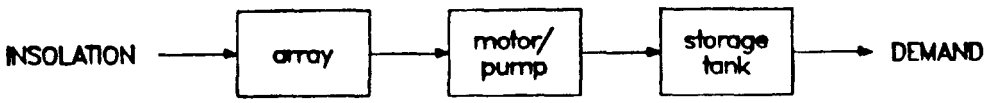

Figure 6. Schematic for direct coupled water pumping system.

There are no components in this system to control the operating voltage. Because the array and motor/pump efficiencies vary with the operating voltage, the designer must perform a single-day simulation to determine the insolation to storage path efficiency η_{in}. To perform the single-day simulation, the designer must first select the building block module and the motor/pump set and specify their performance characteristics. He must also specify the array configuration. The array configuration defines the array area. In cases for which the designer must perform a single-day simulation to determine the path efficiencies, he must first select an array configuration, determine the path efficiencies, and then use equation (3) to calculate POA_0. The S value is determined by interpolating between the four POA_0/S combinations that correspond to the selected tilt angle, obtained from the sizing nomograms. This procedure results in a single POA_0/S combination. The designer must select another array configuration and repeat this procedure to define other POA_0/S combinations. If the selected array configuration results in a POA_0 value that does not lie within the four POA_0 values obtained from the sizing nomograms, that array configuration is discarded.

Component specifications

For the motor/pump set, we will select a 1-hp submersible motor/centrifugal pump set. The operating current-volatge (I-V) curve of the motor is shown in Figure 7. The capacity (Q) of the pump is given by

$$Q = [2\ g\ (H-h)]^{.5}\ A \qquad (7)$$

where H is the total head developed by the pump, h is static head, A is the discharge pipe area, and g is acceleration due to gravity (9.8 m/sec^2). The total head can be approximated from

$$H = H_0\ (RPM/RPM_0)^2 \qquad (8)$$

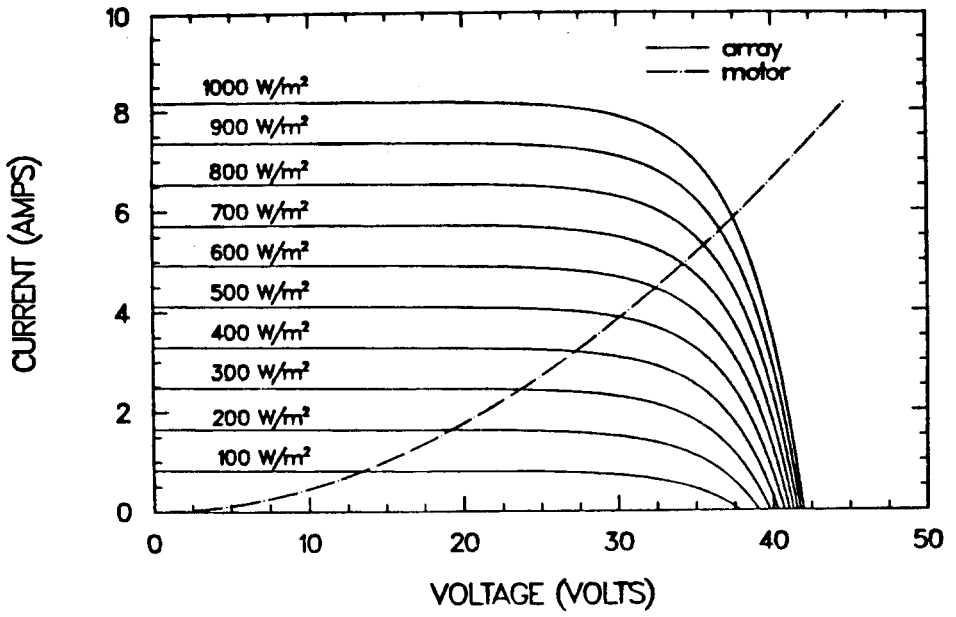

Figure 7. I-V curves for array and motor at 20°C.

where H_0 is the total head at RPM_0. The RPM is given by

$$RPM = [V - (I\ R_{ap})]/K_{sp} \tag{9}$$

where R_{ap} and K_{sp} are characteristics of the motor. The following values were used for the motor/pump parameters.

$A = .000025\ m^2$
$H_0 = 59$ m at 3432 RPM
$R_{ap} = 0.387$ ohms
$K_{sp} = 0.0158$ W/RPM

We will select a 40-watt module with the following characteristics.

area	0.36 m^2
maximum power voltage (Vmp)	16.50
maximum power current (Imp)	2.45
open circuit voltage (Voc)	20.60
short circuit current (Isc)	2.74
temperature coefficients	
voltage (C_v)	0.0783 V/°C
current (C_i)	0.0022 A/°C

Single-day simulation

The system's operating voltage is defined by the intersection of the array and motor I-V curves. The array consists of parallel sets (Npar) of a string of modules in series (Nser). The array's voltage

is the module's voltage multiplied by Nser, and the array's current is the module's current multiplied by Npar. Figure 7 shows array I-V curves (at 20°C) for three parallel sets of two modules in series at various POA insolations. These I-V curves were derived using the module parameters and the I-V model found in "Residential Photovoltaic System Design Handbook" (7). For a given array configuration, the operating voltage and consequently the η_{in} path efficiency (product of the array and motor efficiencies) will vary with POA insolation and temperature.

To determine the η_{in} path efficiency for the design month, the designer must perform a single-day simulation that is representative of an average day. Using techniques found in "Fundamentals of Solar Radiation" (8), we can construct hourly POA insolation values for an average day from the average horizontal insolation, the latitude, and the tilt angle. Table 6 gives the hourly values of POA insolation, operating voltage, the array output, and pump output (hydraulic energy) at various array temperatures for the array configuration represented in Figure 7. The η_{in} path efficiency is the total

Table 6. Single-day simulation for three parallel sets of two modules in series (2.16 m^2).

10°C

hour	POA (W/m^2)	Voltage	Array Output (W)	Pump Output (W)
6-7, 18-19	41	9.8	3.3	0.0
7-8, 17-18	164	17.9	23.6	4.4
8-9, 16-17	337	25.0	67.4	13.9
9-10,15-16	485	30.0	113.7	18.2
10-11,14-15	601	32.8	148.9	20.6
11-12,13-14	672	34.3	168.8	21.8
totals	4598			157.9

η_{in} = 157.9/(4598 x 2.16) = 0.016

20°C

hour	POA (W/m^2)	Voltage	Array Output (W)	Pump Output (W)
6-7, 18-19	41	8.2	2.8	0.0
7-8, 17-18	164	17.4	23.2	4.6
8-9, 16-17	337	25.1	68.0	13.9
9-10,15-16	485	30.0	112.2	18.1
10-11,14-15	601	32.5	144.3	20.3
11-12,13-14	672	33.8	161.7	21.4
totals	4598			156.7

η_{in} = 156.7/(4598 x 2.16) = 0.016

Table 6. Continued

30°C

hour	POA (W/m^2)	Voltage	Array Output (W)	Pump Output (W)
6-7, 18-19	41	6.6	2.3	0.0
7-8, 17-18	164	17.4	23.3	4.7
8-9, 16-17	337	25.1	67.4	13.9
9-10,15-16	485	29.6	109.6	17.9
10-11,14-15	601	32.0	138.1	19.9
11-12,13-14	672	33.2	153.1	20.9
totals	4598			154.8

$$\eta_{in} = 154.8/(4598 \times 2.16) = 0.016$$

hydraulic energy divided by the total POA insolation times the array area. As the array temperature increases, the total array output decreases from 525.7 Wh/day at 10°C to 493.8 Wh/day at 30°C. The increase in array temperature, on the other hand, decreases the operating voltage, which increases the pump's efficiency. The net result is that the pump's output is nearly constant at about 157 Wh/day. Consequently, η_{in} is essentially constant at 0.016. For this system, the array temperature has no effect on η_{in} and can be ignored.

Select array configuration/storage capacity combinations

Single-day simulations were performed for all possible array configurations from a total of 1 to 20 modules. Table 7 lists the array configuration/storage capacity combinations that give POA_0 values within the four POA_0s obtained from the sizing nomograms. If there are no overriding constraints on either the array size or storage capacity, the designer would choose the least costly array configuration/storage capacity combination.

Table 7. Possible array configuration/storage capacity combinations for water pumping system.

# modules (Nser,Npar)	A (m^2)	η_{in}	POA_0 (kWh/m^2-day)	S	Capacity (m^3)
6 (2,3)	2.16	0.016	3.94	2.16	21.6
8 (2,4)	2.88	0.014	3.38	1.78	17.8
9 (3,3)	3.24	0.011	3.82	2.08	20.8
10 (2,5)	3.60	0.012	3.15	1.62	16.2
12 (3,4)	4.32	0.010	3.15	1.62	16.2
12 (4,3)	4.32	0.008	3.94	2.16	21.6
15 (5,3)	5.40	0.007	3.60	1.93	19.3

SUMMARY

We have presented a quantitative sizing procedure for stand-alone PV/storage systems. The technique involves the following four steps.

Step One. Define Site- and Application-Specific Parameters.

Site-specific parameters
- average horizontal insolation (December or June)
- latitude.

Application-specific parameters
- average daily demand
- loss-of-load probability (LOLP).

Step Two. Determine Array Sizes in terms of Design Insolations.

- four sets of design insolations.
- each sets contains a series of five design insolations, one for each tilt angle option.
- select tilt angle.

Step Three. Determine Storage Capacities in terms of Days of Storage.

- four values of days of storage, one for each set of design insolations.

Step Four. Translate Design Insolations and Days of Storage into Array Areas and Storage Capacities.

- define system configuration and component specifications.

- determine path efficiencies as defined by equations (1) and (2).

- use equations (3) and (4) to select array configurations/storage capacity combinations.

REFERENCES

1. "SOLMET - Hourly Solar Radiation-Surface Meteorological Observations, Volume I - Users Manual," TD-9724, August 1978.

2. Liu, B.Y.H., and Jordan, R.C., "The Interrelationships and Characteristic Distribution of Direct, Diffuse, and Total Radiation," SOLAR ENERGY, Vol. 4, No. 3, 1960, pp. 1-19.

3. Klein S.A., and Beckman, W.A., "Loss-of-Load Probabilities for Stand-Alone Photovoltaic Systems," Proc. SOLAR 87 Conference, July 12-16, 1987, Portland, Oregon.

4. Knapp, C.L., Stoffel, T.L., and Whitaker, S.D., "Insolation Data Manual," SERI/SP-755-789, Solar Energy Information Data Bank, Solar Energy Research Institute, Golden, Colarado, October 1980.

5. Lof, G.O.D., Duffie, J.A., and Smith, C.O., "World Distribution of Solar Radiation," Report No. 21, Engineering Experiment Station, College of Engineering, University of Wisconsin, Madison, Wisconsin, 1966.

6. Major, G., et al., "Meteorological Aspects of the Utilization of Solar Radiation as an Energy Source, Annex - World Maps of Relative Global Radiation," Technical Note No. 127, WHO-No. 577, Meteorological Service of the Hungarian People's Republic, Budapest, Hungary, 1981.

7. Russell, M.C., "Residential Photovoltaic System Design Handbook," DOE/ET/20279-255, Massachusetts Institute of Technology, Northeast Residential Experiment Station, Concord, Massachusetts, April 1984.

8. Boes, E.C., "Fundamentals of Solar Radiation," SAND 79-0490, Sandia National Laboratories, Albuquerque, New Mexico, December 1979.

APPENDIX A1.

SIZING NOMOGRAMS FOR SIZE SET 1

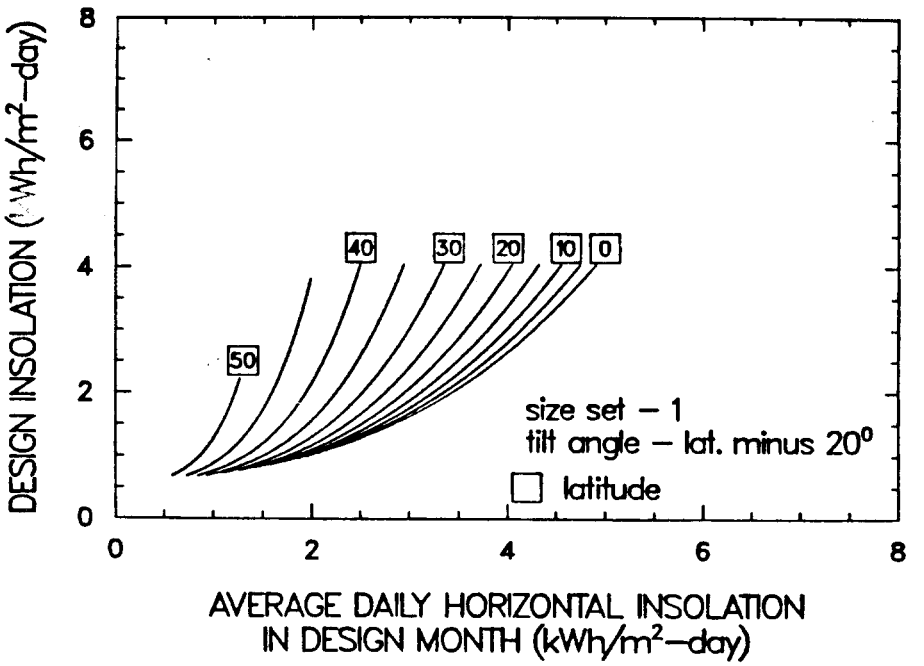

Figure A1a. Array-sizing nomogram.
Size set 1 - tilt angle = latitude minus 20°

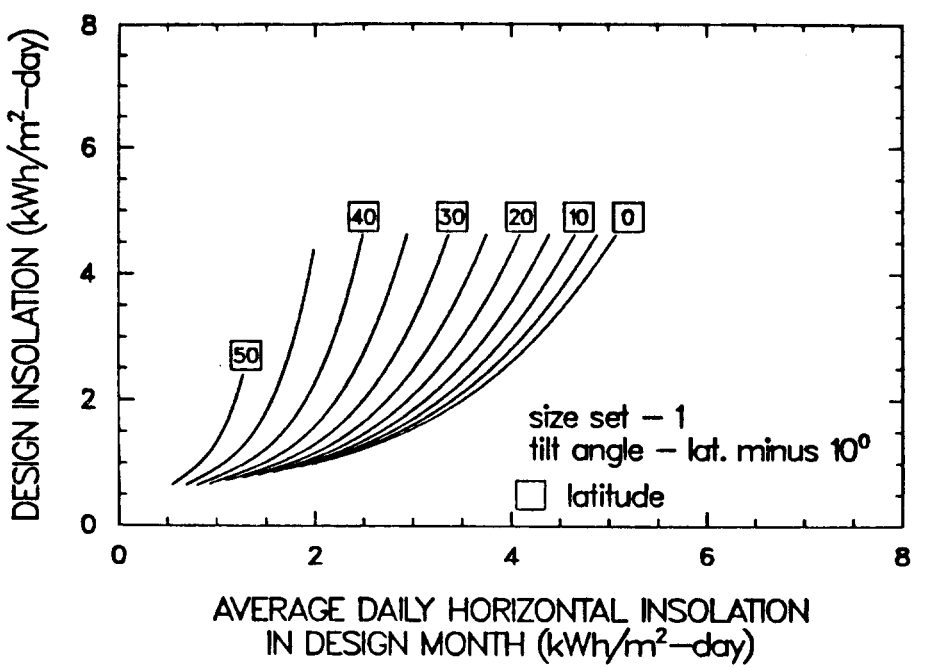

Figure A1b. Array-sizing nomogram.
Size set 1 - tilt angle = latitude minus 10°

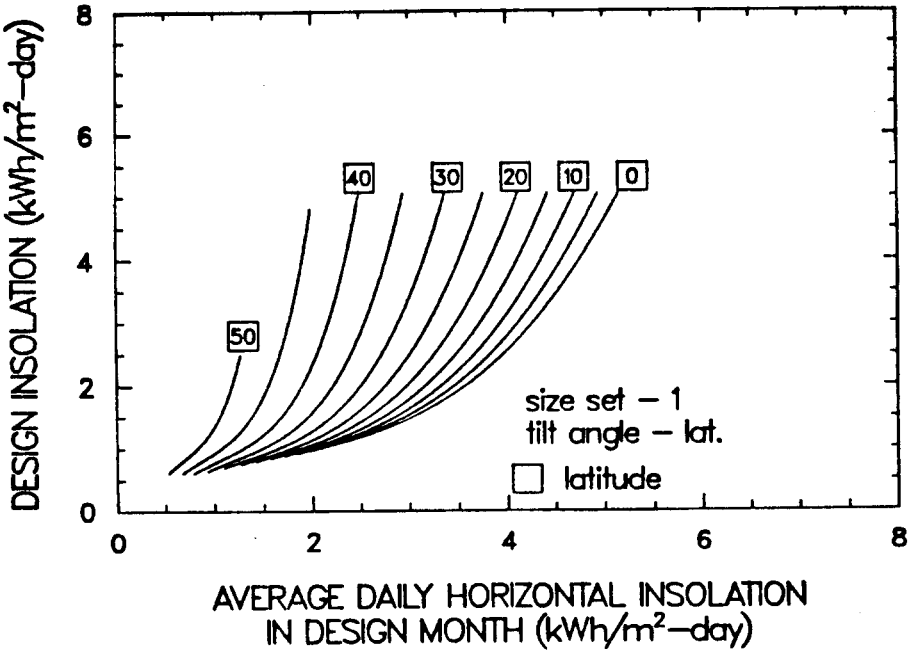

Figure A1c. Array-sizing nomogram.
Size set 1 - tilt angle = latitude

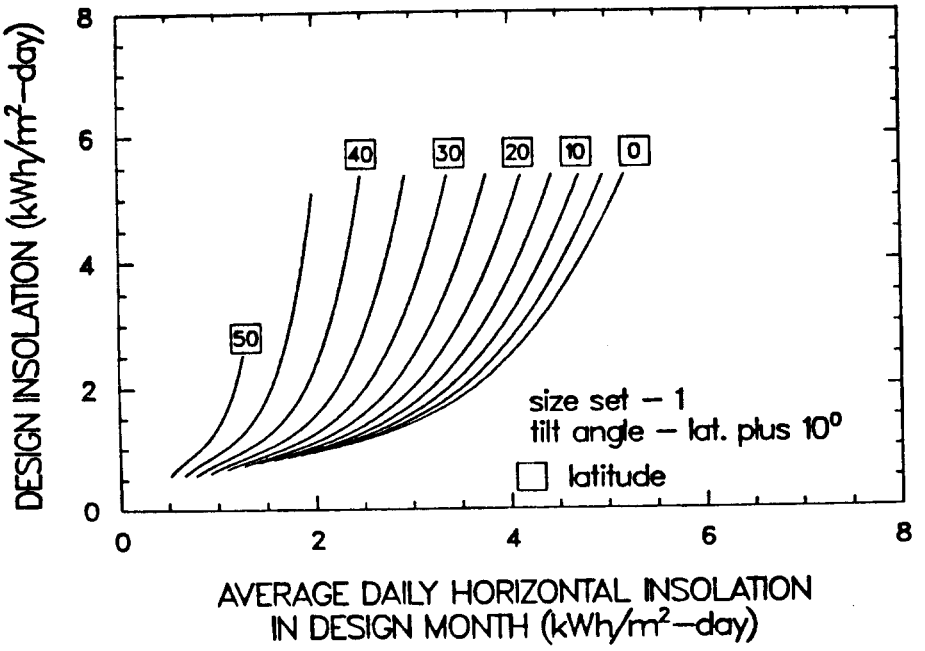

Figure A1d. Array-sizing nomogram.
Size set 1 - tilt angle = latitude plus 10°

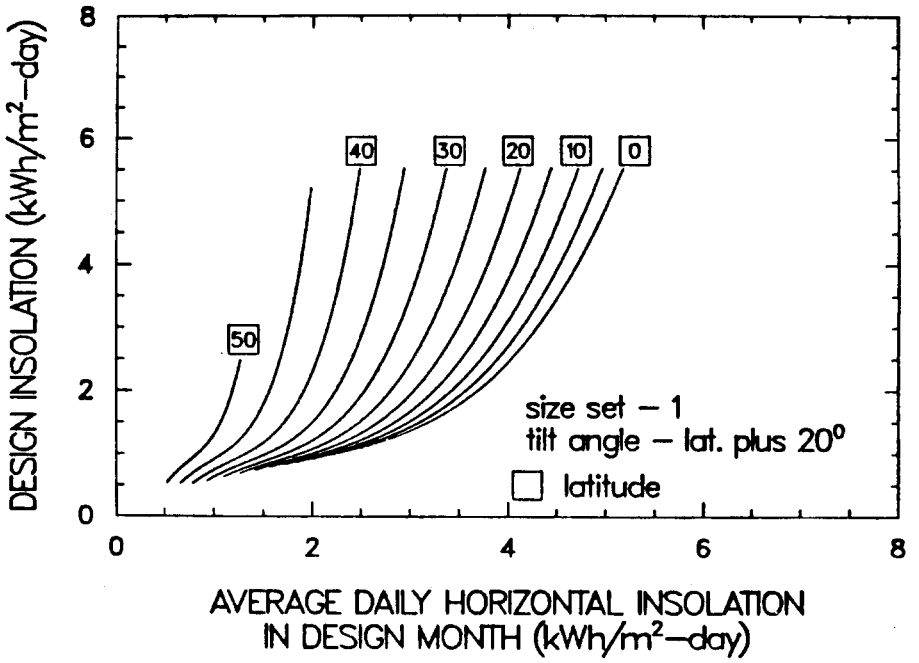

Figure A1e. Array-sizing nomogram.
Size set 1 - tilt angle = latitude plus 20°

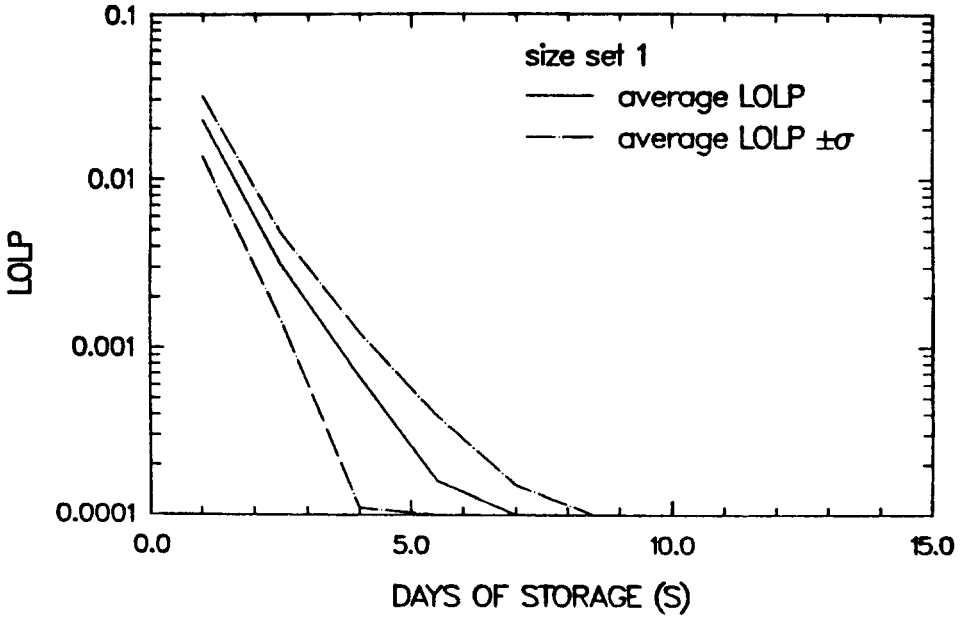

Figure A1f. Storage-sizing nomogram.
Size set 1

APPENDIX A2.

SIZING NOMOGRAMS FOR SIZE SET 2

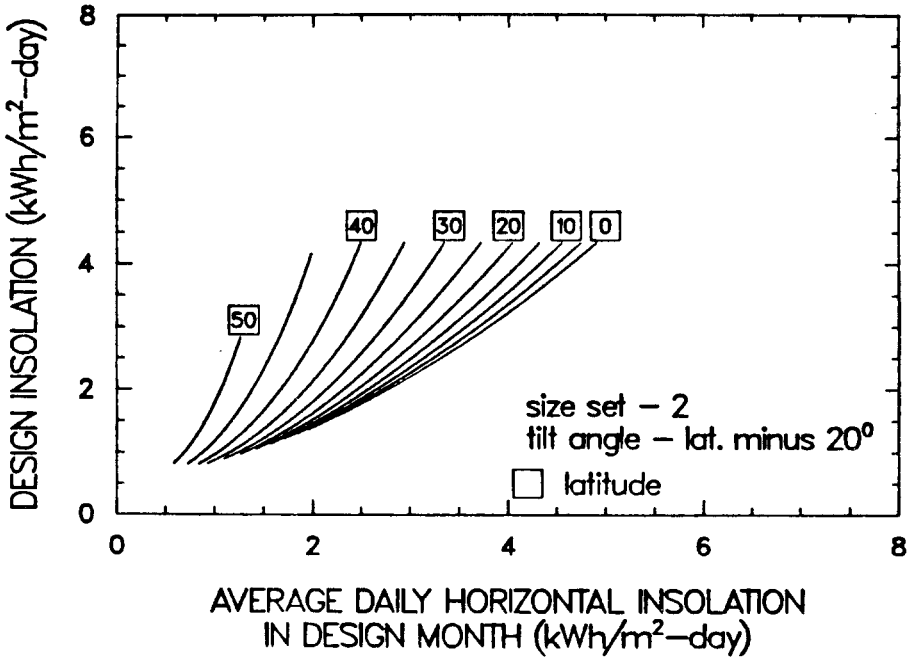

Figure A2a. Array-sizing nomogram.
Size set 2 - tilt angle = latitude minus 20°

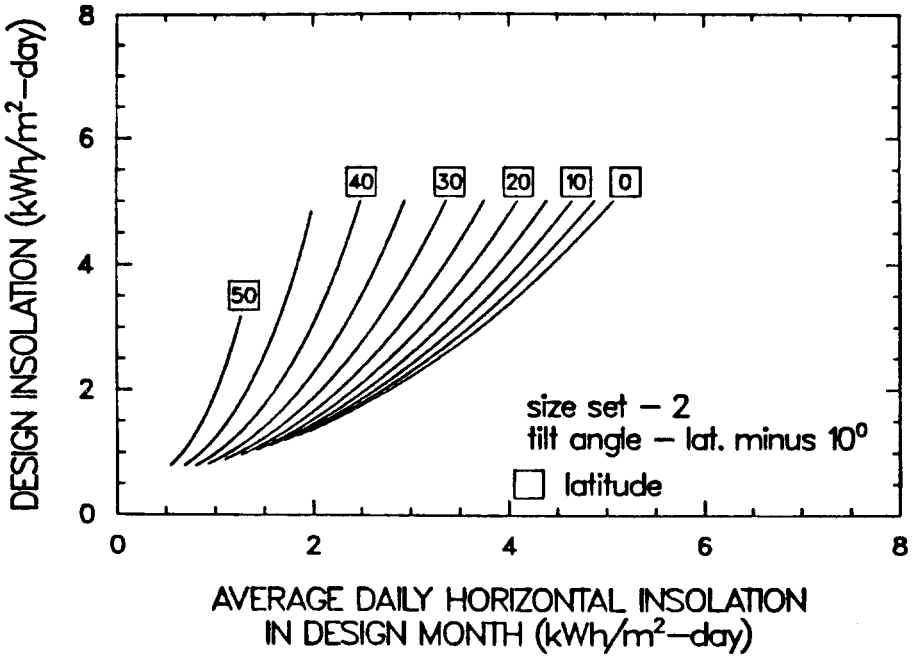

Figure A2b. Array-sizing nomogram.
Size set 2 - tilt angle = latitude minus 10°

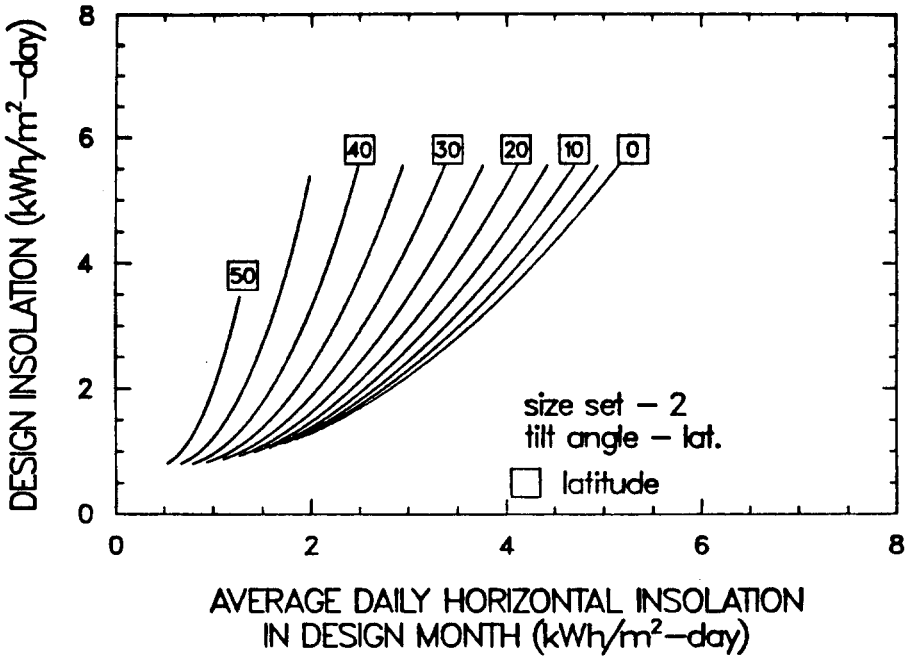

Figure A2c. Array-sizing nomogram.
Size set 2 - tilt angle = latitude

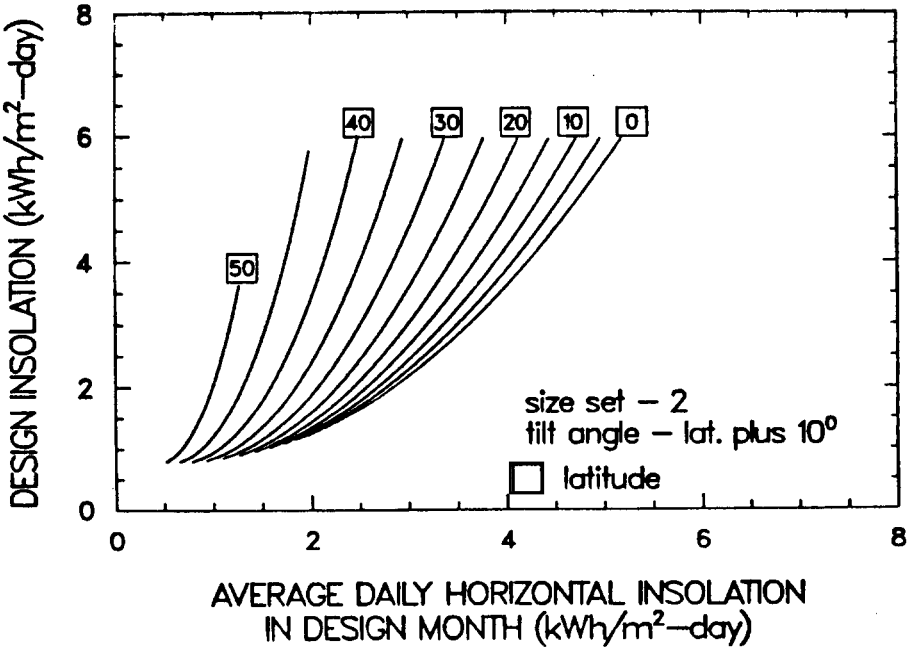

Figure A2d. Array-sizing nomogram.
Size set 2 - tilt angle = latitude plus 10°

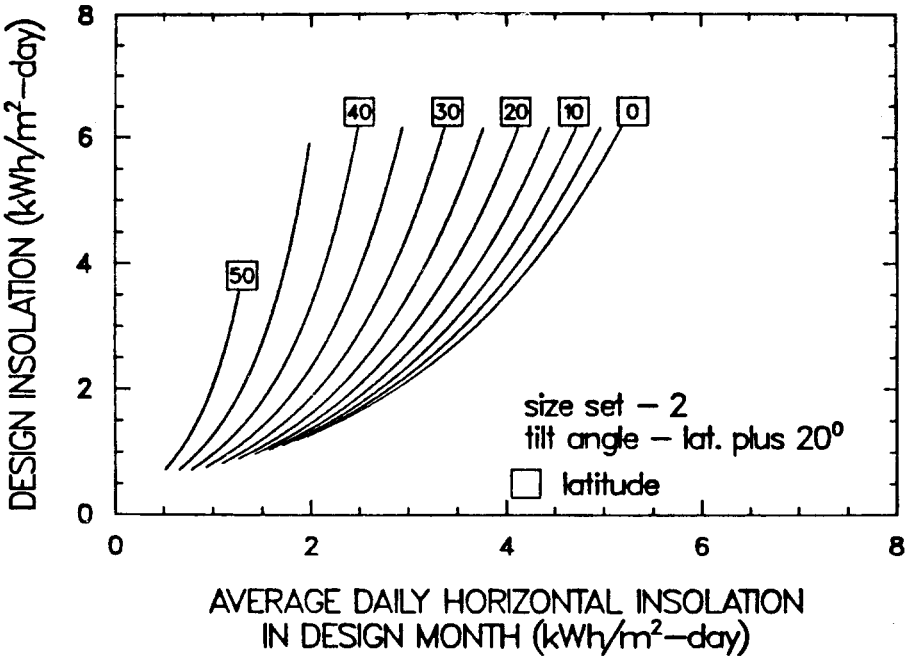

Figure A2e. Array-sizing nomogram.
Size set 2 - tilt angle = latitude plus 20°

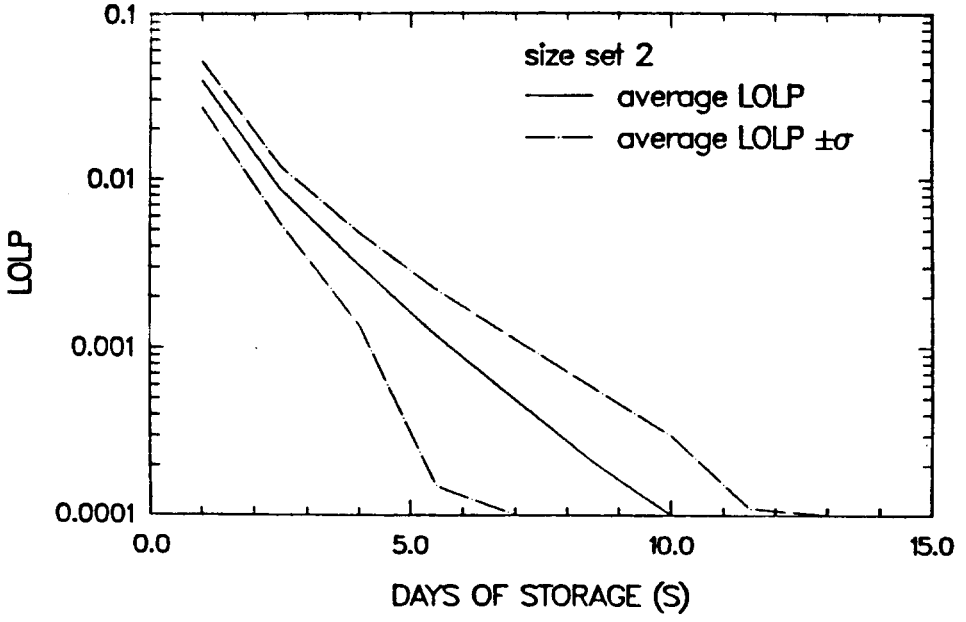

Figure A2f. Storage-sizing nomogram.
Size set 2

APPENDIX A3.

SIZING NOMOGRAMS FOR SIZE SET 3

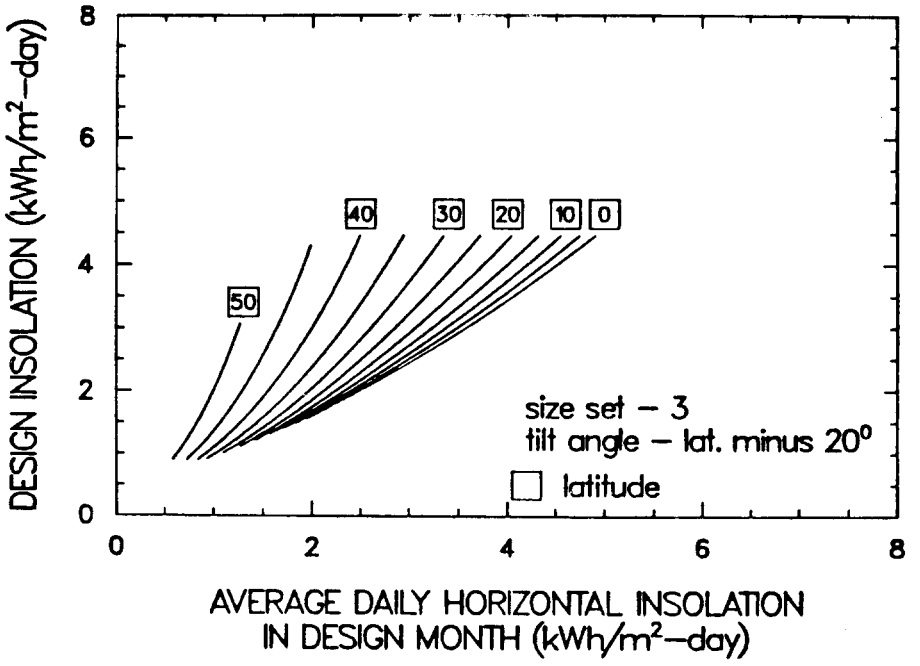

Figure A3a. Array-sizing nomogram.
Size set 3 - tilt angle = latitude minus 20°

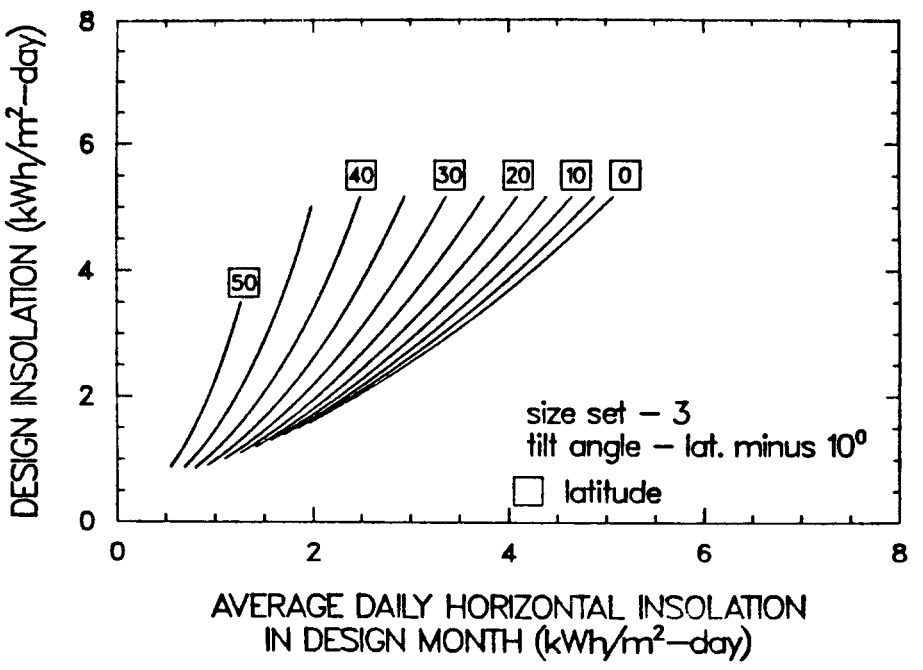

Figure A3b. Array-sizing nomogram.
Size set 3 - tilt angle = latitude minus 10°

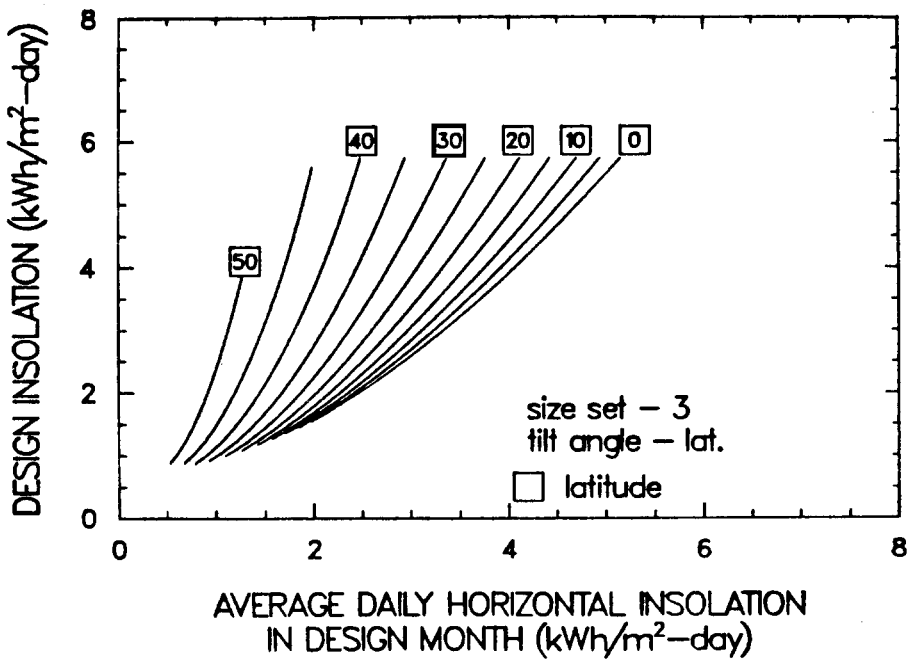

Figure A3c. Array-sizing nomogram.
Size set 3 - tilt angle = latitude

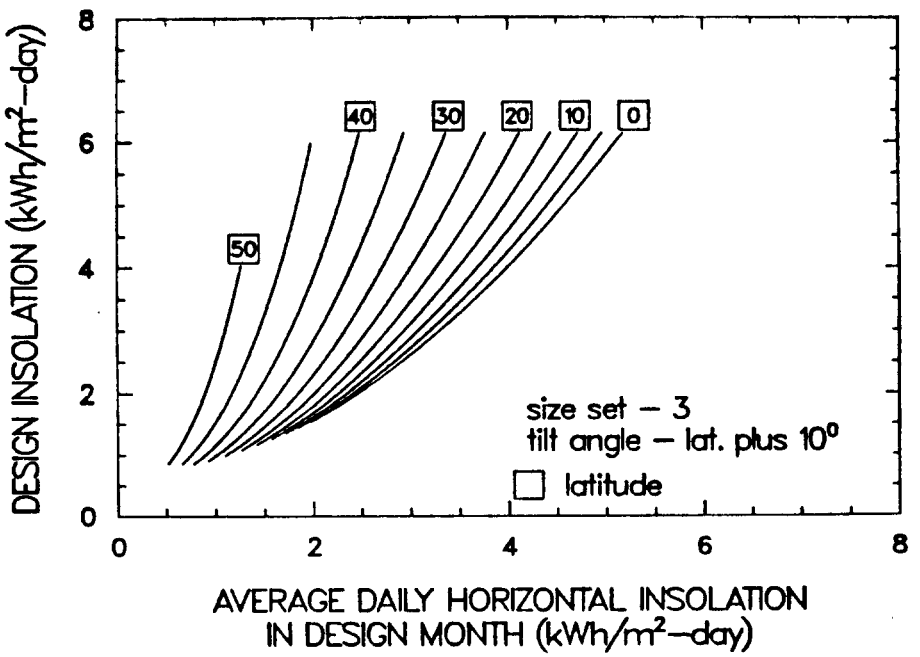

Figure A3d. Array-sizing nomogram.
Size set 3 - tilt angle = latitude plus 10°

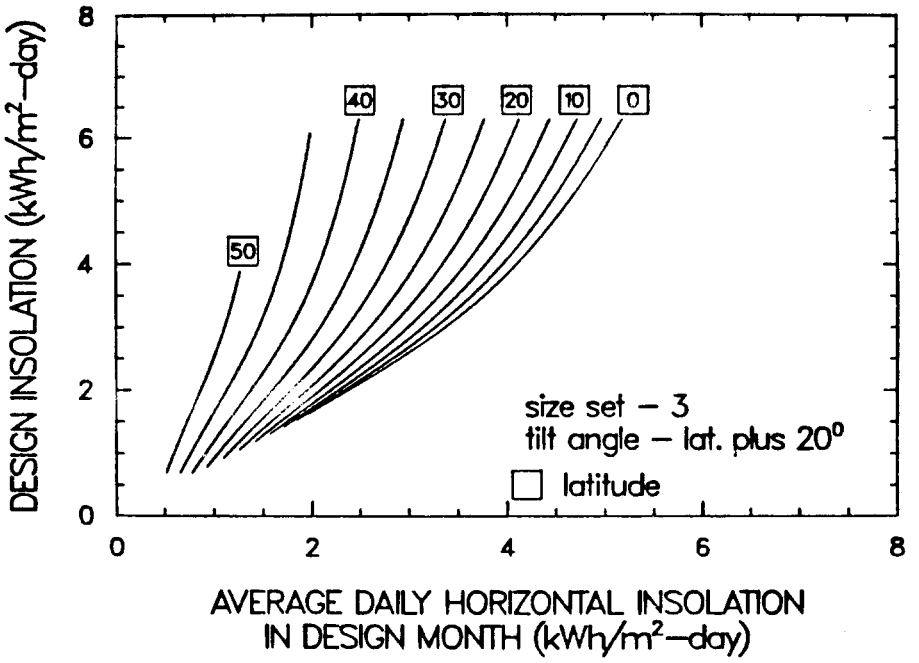

Figure A3e. Array-sizing nomogram.
Size set 3 - tilt angle = latitude plus 20°

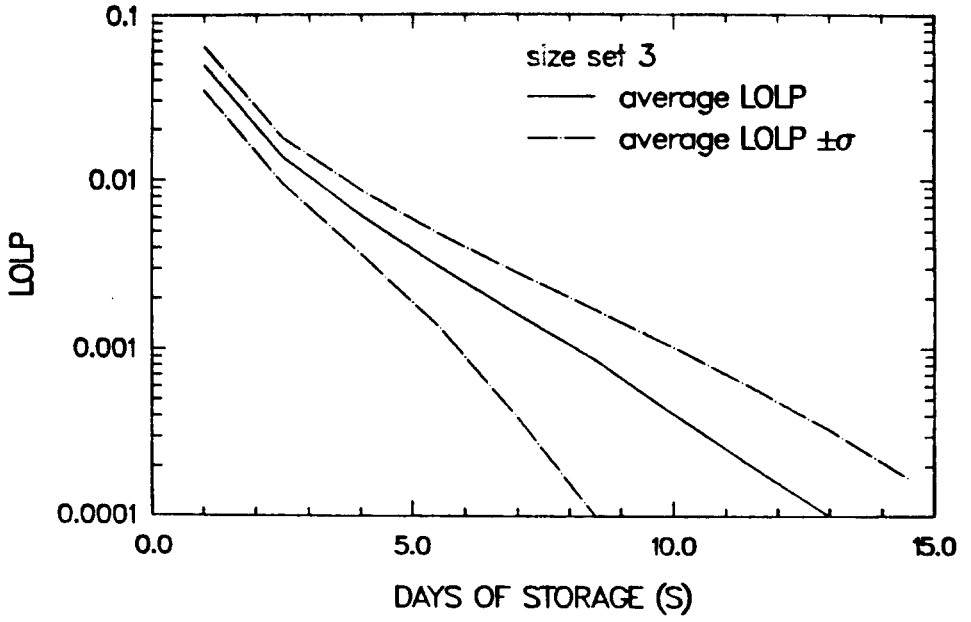

Figure A3f. Storage-sizing nomogram.
Size set 3

APPENDIX A4.

SIZING NOMOGRAMS FOR SIZE SET 4

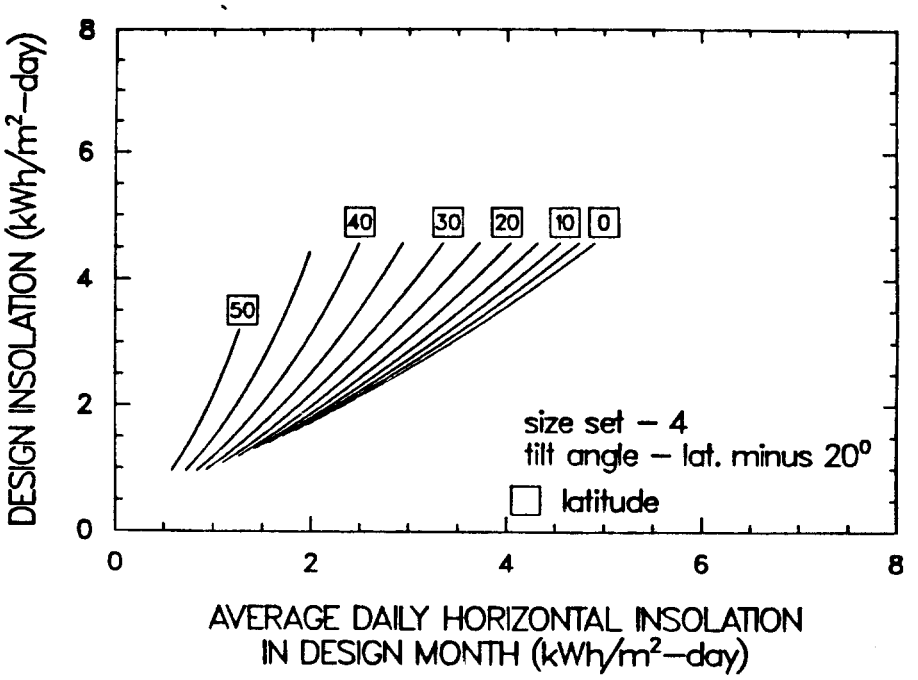

Figure A4a. Array-sizing nomogram.
Size set 4 - tilt angle = latitude minus 20°

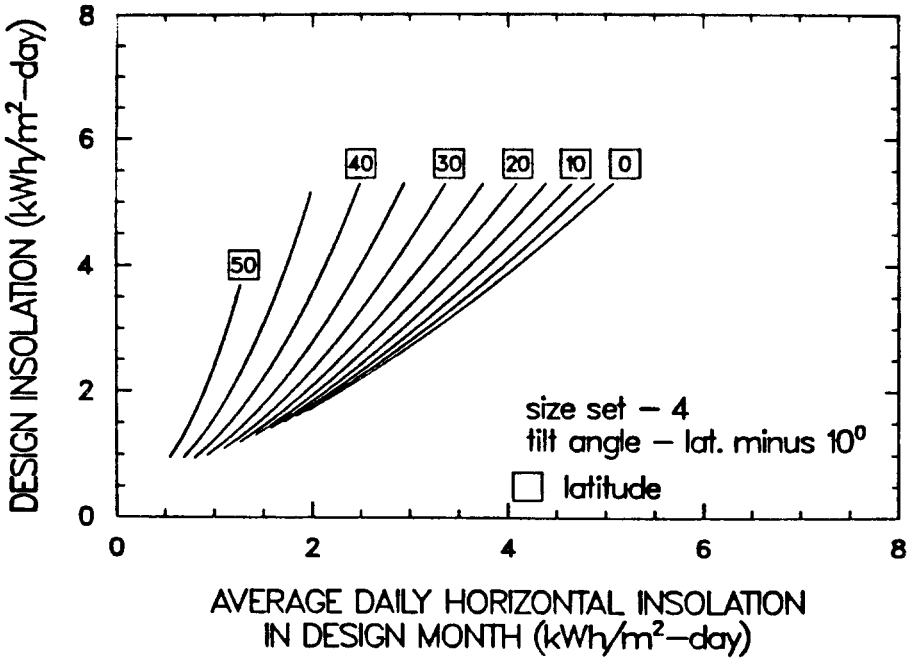

Figure A4b. Array-sizing nomogram.
Size set 4 - tilt angle = latitude minus 10°

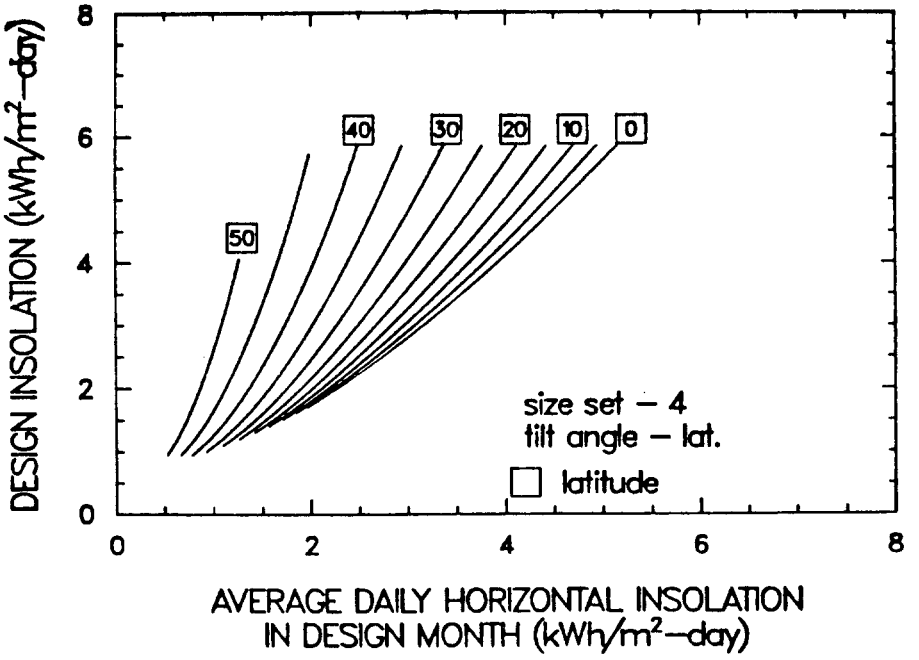

Figure A4c. Array-sizing nomogram.
Size set 4 - tilt angle = latitude

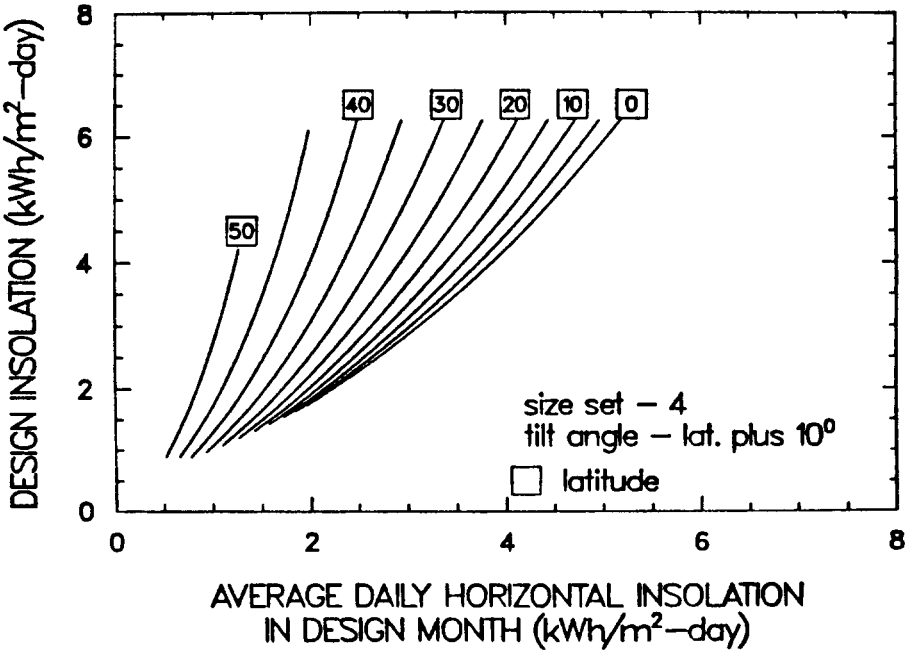

Figure A4d. Array-sizing nomogram.
Size set 4 - tilt angle = latitude plus 10°

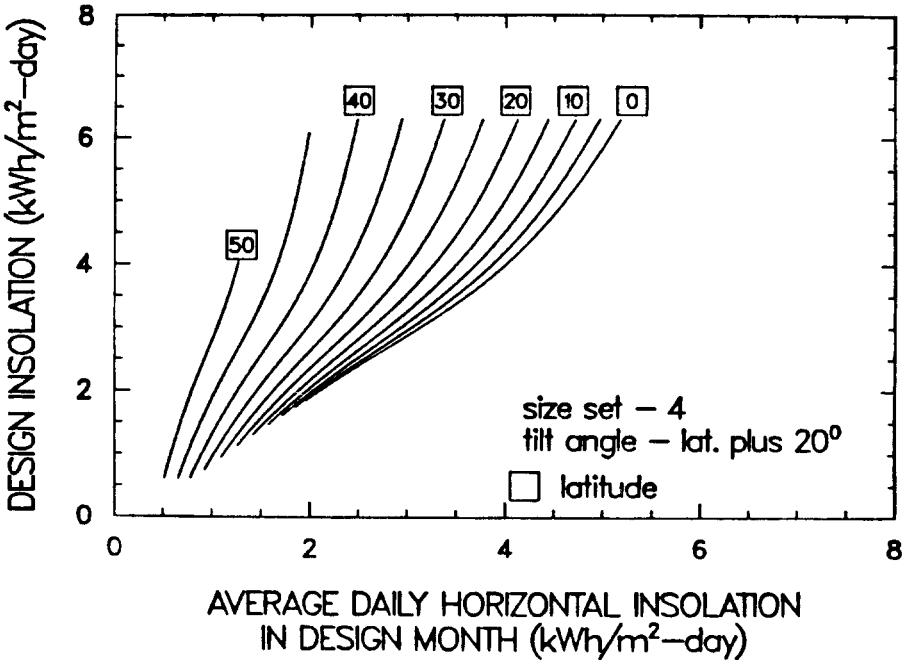

Figure A4e. Array-sizing nomogram.
Size set 4 - tilt angle = latitude plus 20°

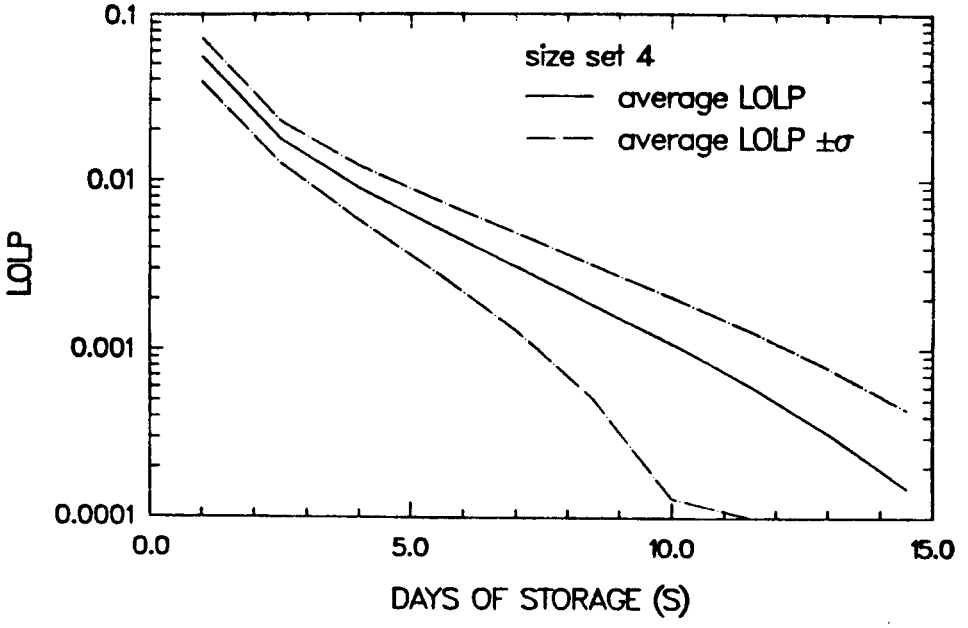

Figure A4f. Storage-sizing nomogram.
Size set 4

APPENDIX B. Development of Sizing Nomograms

Basis of Loss-of-Load Simulation Model

The usefulness of the sizing nomograms depends on two factors; the accuracy and applicability of the simulation model. If the model is accurate, but only valid for one system, the nomograms are of little use. The same result holds if the model is applicable to any system, but is grossly inaccurate. Normally, as a performance model becomes more generic, it becomes less accurate. There is, however, an acceptable compromise.

Simulation model research at Sandia has shown that the method used to calculate the POA insolation dominates the accuracy of the performance predictions (1). The effects of other factors, such as how the array efficiency varies with temperature and insolation, tend to be second order. Therefore, as long as the POA insolation calculations are accurate, one can use constant efficiencies for the components without sacrificing accuracy. This does not imply that the values of the component efficiencies are unimportant. What it does mean is that if appropriate values are used for the constant efficiencies, the difference between LOLPs predicted using hourly calculated efficiencies and the constant efficiencies will be negligible. This approach is acceptable for most stand-alone systems. In this analysis, the appropriate values for the efficiencies are the average daily efficiencies for the design month.

Derivation of Loss-of-Load Simulation Model

The use of constant component efficiencies allows one to develop an LOLP simulation model in which all system-specific parameters are incorporated into two user-supplied parameters. The system is modeled by grouping the components into three subsystems, an array subsystem, a storage subsystem, and a demand subsystem, in such a way that the energy or product flows in and out of the storage subsystem can be represented by

$$S_i = S_{i-1} + (POA_i/POA_0) - LF_{hr} \qquad (1B)$$

where S_i is the normalized stored energy available for hour i, POA_i is the plane of array insolation for hour i, POA_0 is the design insolation, LF_{hr} is the fraction of the daily energy demand that occurs during hour i, and S_{i-1} is the normalized stored energy available from the previous hour. Equation (1B) is derived below.

The amount of energy generated by the array subsystem (Ea_i) is given by

$$Ea_i = POA_i \; A \; \eta_a \qquad (2B)$$

where A is the array area, and η_a is the efficiency of the array subsystem. The energy flow in and out of the storage subsystem is

given by

$$C_i = C_{i-1} + (Ea_i\ f\ \eta_{s,in}) - [LF_{hr}\ El/\eta_l - Ea_i\ (1-f)]/\eta_{s,out} \tag{3B}$$

where C_i and C_{i-1} are the available stored energies at the current and previous time steps, El is the daily energy demand, η_l is the average daily load subsystem efficiency, $\eta_{s,in}$ and $\eta_{s,out}$ are storage and retrieval efficiencies of the storage subsystem, and f is the fraction of Ea_i that is added to storage.

The factor f was set equal to 1 which forces all energies to flow through the storage subsystem. As we shall see later, this choice of f allows the derivation of equation (1B). Although the value of 1 for f is does representative of the actual energy flows, it does not introduce error into the LOLP. Equation (3B) then reduces to

$$C_i = C_{i-1} + Ea_i\ \eta_{s,in} - LF_{hr}\ El/(\eta_l\ \eta_{s,out}) \tag{4B}$$

At this point, it is convenient to introduce the concept of the design insolation, POA_0, from which the array size is determined. It is defined as

$$El/(\eta_{out}) = POA_0\ A\ \eta_{in}. \tag{5B}$$

The parameter η_{in} is referred to as the path efficiency from insolation to storage and is defined as

$$\eta_{in} = \eta_a\ \eta_{s,in}. \tag{6B}$$

The parameter η_{out} is referred to as the path efficiency from storage to demand and is defined as

$$\eta_{out} = \eta_{s,out}\ \eta_l. \tag{7B}$$

By solving equation (5B) for A η_a and substituting into equation (2B), we obtain

$$Ea_i\ \eta_{s,in} = POA_i/POA_0\ (El/\eta_{out}) \tag{8B}$$

Substituting equations (7B) and (8B) into equation (4B) and dividing through by El/η_{out}, we obtain

$$S_i = S_{i-1} + (POA_i/POA_0) - LF_{hr} \tag{9B}$$

where S_i and S_{i-1} are defined as

$$S_i = C_i\ /\ (El/\eta_{out}) \tag{10B}$$

and are subject to the following bounds

$$0 \le S_i \le S_0 \tag{11B}$$

where S_0 is the normalized storage capacity.

The loss-of-load for hour i (LOL_i) represents the amount of

load not satisfied and is defined as

$$LOL_i = \begin{cases} 0 & \text{if } E_i \geq LF_{hr} \\ LF_{hr} - E_i & \text{if } E_i < LF_{hr} \end{cases} \tag{12B}$$

where E_i is the energy available for the load and is defined as

$$E_i = S_i + POA_i/POA_0. \tag{13B}$$

The long-term loss-of-load probability (LOLP) is the average of the LOL_i values and is estimated as shown in Figure B1.

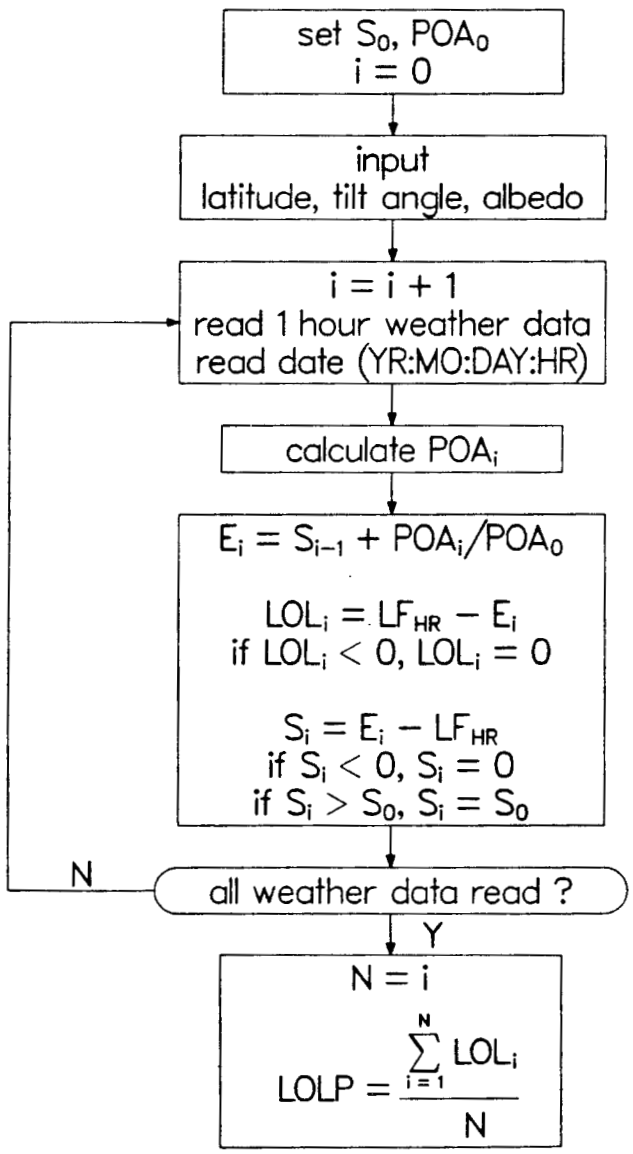

Figure B1. Calculation of loss-of-load probability (LOLP)

Testing of the Loss-of-Load Simulation Model

The loss-of-load (LOL) simulation model was verified by comparing its' LOLP values against LOLP values estimated using the proven PVFORM simulation model (2). PVFORM consists of subroutines that estimate array efficiency, battery charge and discharge efficiencies, and inverter efficiency. The array efficiency varies with cell temperature which depends on wind speed, ambient temperature, and insolation. The battery charge and discharge efficiencies depend on battery state-of-charge and the inverter efficiency depends on the load-factor. All these efficiencies can vary significantly. This comparison is therefore of valid test of using constant component efficiencies. The parameters required to run PVFORM were set as shown in Table B1.

TABLE B1. PVFORM Parameters.

Array	
INOCT (installed operating cell temperature)	48°C
Reference efficiency at INOCT	10%
Maximum power temperature coefficient (default)	-0.4%/°C
Size	See Table B2
Battery	
Maximum charge efficiency	80%
Maximum discharge efficiency	90%
Minimum state-of-charge	0.2
Capacity	see Table B2
Load	
Total daily demand (constant)	120 kWh ac
Peak demand (default)	9 kW
Minimum demand (default)	3 kW
Hourly profile (default)	residential
Inverter	
Rating	10 kW ac
Full-load efficiency	92%

Comparisons were made with data from four sites, Albuquerque, NM, Charleston, TN, Medford, OR, and Seattle, WA. The LOL simulation model was run with the constant array efficiencies given in Table B2, battery charge and discharge efficiencies of 80 and 90 %, a minimum state-of-charge of 0.2, and an inverter efficiency of 91.2% with the residential hourly load profile. The plane-of-array calculations in PVFORM and the LOL simulation model are identical. The resulting LOLP values are shown in Table B2.

LOLPs were estimated at small and large battery capacities at each site to give comparisons at high and low values of LOLP. In all cases, the error induced by using constant efficiencies and a value of 1 for f is on the order of ± 50% and is within the uncertainty associated with the LOLP values given by this sizing technique. This

test shows that the LOL simulation model is accurate when correct values for the average daily path efficiencies are used. Guidelines for determining these path efficiencies are given in the main body of this report.

Table B2. Comparison of LOL simulation model and PVFORM

Site	Array Size* (m^2)	Battery Cap (kWh)	LOL simulation	PVFORM
Albuquerque	365.0	150	0.038	0.027
	(10.7)	600	0.0036	0.0012
Charleston	585.0	150	0.077	0.065
	(10.1)	750	0.0035	0.0018
Medford	1266.0	150	0.045	0.039
	(9.9)	750	0.0050	0.0033
Seattle	1825.0	158	0.090	0.080
	(8.2)	750	0.024	0.012

* Number in parentheses is the average daily array efficiency in the design month as determined using PVFORM.

Generation of Sizing Nomograms

Basis of sizing nomograms

Given a value for POA_0 and the SOLMET data from one site, one can generate a curve of LOLP as a function of S_0 using the LOL simulation model described above. These analyses were performed over a range of S_0 values from 1 to 15. The lower value represents the minimum storage required for a stand-alone system, and the upper value represents the amount of storage at which LOLP approaches zero. We found that it was possible to define a set of POA_0s, one for each site, so that the deviation between the LOLP curves from all twenty sites became very small and the POA_0 values could be correlated with the average December POA insolation (3). This result formed the basis for generating sizing nomograms in which the array size is given by readily available insolation data, and the storage capacity is given by the desired LOLP.

This preliminary work was done assuming that the array was tilted at latitude. Furthermore, insolation data are most commonly available as horizontal insolation and not POA insolation. Our first objective was to generate sizing nomograms that were applicable for a range of tilt angles from latitude minus 20° to latitude plus 20° and required horizontal insolation data as input instead of POA insolation data. A second objective was to generate nomograms that allow the designer to choose from several combinations of array size/storage capacity that give the same LOLP. These combinations would range from large array and small storage capacity to small array size and large storage capacity allowing the designer to select

the most cost-effective combination depending on the cost of the array and storage. The next section describes the approach used to meet these objectives.

Method used to generate nomograms

The overall approach was to define an appropriate correlation between the POA_0 and average December POA insolations and then structure a parameter estimation routine to search for correlation parameters that minimize the deviation between the LOLP curves. The correlation was defined as

$$POA_0 = a_0 + a_1 POA + a_2 POA^2 - a_3 POA^3, \qquad (14B)$$

where $a_0 \ldots a_3$ are the correlation parameters. To eliminate the POA insolation as an input to the routine, it was related to the average December horizontal insolation using the method of Liu and Jordan (4).

The routine was structured as shown in Figure B2. The sequence of steps shown in Figure B2. are described below.

Step 1. Select values for the tilt and S_0. The resulting correlations will only be valid for the selected tilt angle.

Step 2. Use the LOL simulation model and SOLMET data to generate values of LOLP for a range of POA_0 values and a preset value of S_0. The values of LOLP define discrete functions (f_n)

$$LOLP_n = f_n(POA_0, S_0), \qquad (15B)$$

where the subscript n denotes the site. The functions f_n are made up of 350 LOLP values corresponding to POA_0 values from .2 to 7 kWh at an interval of .2 kWh.

Step 3. Calculate an average December POA insolation value for each site from the average horizontal insolation, tilt angle of the array, latitude of the site, and the ground albedo. The average horizontal insolations were derived directly from the SOLMET data. The ground albedo values had no discernible effect on the correlations. A value of .3 was used for all sites.

Step 4. Input an initial estimate of $a_0 \ldots a_3$.

Step 5. Calculate a POA_0 value for each site using equation (14B) and the current values for $a_0 \ldots a_3$.

Step 6. Determine an LOLP value for each site that corresponds to the POA_0 value calculated in Step 5 using the functions f_n defined in Step 2. The LOLP values are determined by interpolating between the points in f_n.

Step 7. Calculate the least squares difference between the $LOLP_n$ values and a preset value $LOLP_0$. In this type of analysis, one normally calculates an average LOLP value and uses that value to calculate the difference. This technique

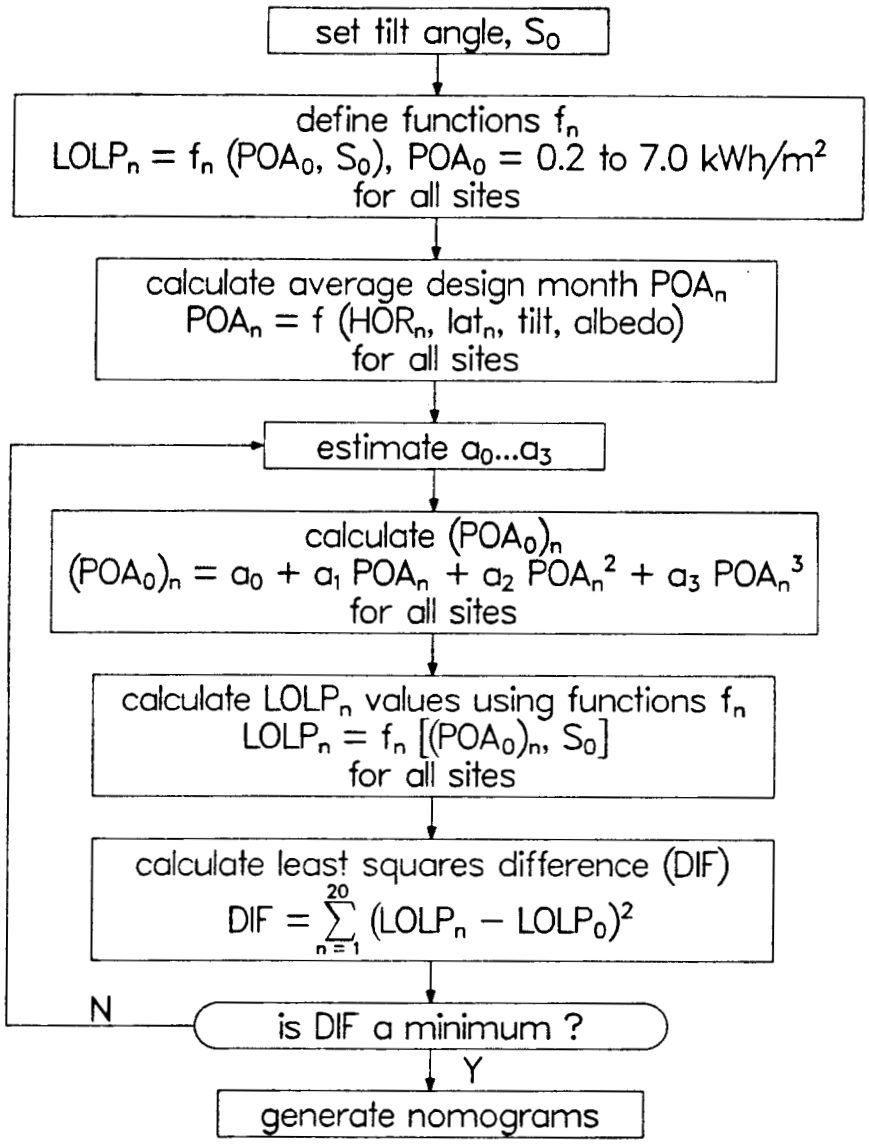

Figure B2. Structure of parameter estimations routine.

cannot be used in this analysis because the LOLP values go to zero as POA_0 decreases (i.e., the array size increases). If the difference was calculated from the average, the parameter estimation routine would always give the trivial solution in which $(POA_0)_n = 0$, $LOLP_n = 0$, and the difference = 0.

The approach used in this analysis also provides a convenient means to generate correlations for various array/storage combinations. By fixing $LOLP_0$ at some value and increasing S_0, we force the correlation to generate higher POA_0 values (smaller array sizes). The net result

is the same $LOLP_n$ values at larger storage capacities (larger S_0s) and smaller array sizes (larger POA_0s). Correlation were generated with S_0 set equal to 2.5, 4.0, 5.5, and 7.0.

Note that the difference is only calculated one S_0 value rather than over the entire range of S_0 values. This greatly simplified coding and executing the parameter estimation routine and did not reduce the accuracy of the correlations.

NOTE - Step 8 was performed using a function minimization routine provided by R. J. Hanson, Sandia National Laboratories. A description of the technique can be found elsewhere (5).

Step 8. Determine if the differences are minimized. If they are, go to Step 9. If not, estimate new values of a_0 ... a_3 and return to Step 4.

Step 9. The current values for a_0 ... a_3 define the correlation for the current tilt angle. This correlation is used to generate the array-sizing nomograms. The storage-sizing nomograms are generated by calculating LOLP values for S values from 1 to 14.5 using the LOL simulation model and the POA_0 values defined by the correlation.

Four sets of correlations were defined by twenty runs of the parameter estimation routine. The four sets represent four array/storage combinations generated by varying the value of S_0. Each set contains five correlations corresponding to tilt angles of latitude plus -20, -10, 0, 10, and 20°. The parameters a_0 ... a_3 for all twenty correlations are given in Table B3. The tilt angle had no effect on the storage-sizing nomograms. Each set of nomograms therefore has a single storage-sizing nomogram that represents all tilt angles.

Table B3.
Correlation Parameters

Size Set	Tilt Set	a_0	a_1	a_2	a_3
1	1	0.446	0.256	-0.086	0.0600
	2	0.169	0.679	-0.268	0.0703
	3	-0.003	0.882	-0.337	0.0690
	4	-0.137	1.011	-0.375	0.0674
	5	-0.266	1.136	-0.413	0.0680
2	1	0.554	0.026	0.232	-0.0018
	2	0.509	0.130	0.143	0.0079
	3	0.810	-0.251	0.252	-0.0049
	4	0.807	-0.233	0.221	-0.0019
	5	0.245	0.488	-0.044	0.0239
3	1	0.362	0.376	0.157	0.0001
	2	0.360	0.368	0.138	0.0009
	3	0.596	0.066	0.225	-0.0087
	4	0.472	0.237	0.144	-0.0003
	5	-0.605	1.554	-0.311	0.0433
4	1	0.322	0.492	0.142	-0.0007
	2	0.463	0.297	0.199	-0.0088
	3	0.527	0.221	0.209	-0.0101
	4	0.120	0.744	0.011	0.0101
	5	-1.328	2.405	-0.532	0.0599

REFERENCES

1. Menicucci, D.F., and Fernandez, J.P., "Verification of Photovoltaic System Modeling Codes Based on System Experimental Data", The Proceedings of the Seventeenth IEEE Photovolatics Specialists Conference, Kissimee, Florida, May 1984.

2. Menicuucci, D.F., "PVFORM - A New Approach to Photovoltaic System Performance Modelling," Proceedings of the Eighteenth IEEE Photovoltaic Specialists Conference, Las Vegas, Nevada, October 1985.

3. Chapman, R. N., "Design Considerations for Stand-Alone Photovoltaic", Proceedings of the 1986 International Symposium on Solar and Renewable Energy, March 23-26, Cairo, Egypt, paper ASRE-126.

4. Liu, B. Y. H., and Jordan, R. C., "Daily Insolation of surfaces tilted towards the equator", Trans ASHRAE, 526-541 (1962).

5. Hanson, R. J. and Krogh, F. T., "A New Algorithm for Constrained Nonlinear Least Squares Problems", submitted for publication in ACM-TRANS. Math. Software, Sandia National Laboratories, Albuquerque, NM 87185

Distribution - DAC

Abacus Controls, Inc.
Attn: Mr. George O'Sullivan
P. O. Box 893
Somerville, NJ 08876

Acurex Corporation
Attn: Dan Rosen
555 Clyde Avenue
P. O. Box 7555
Mountain View, CA 94039

AEG Corporation
Attn: Walter J. O'Neill
Bldg. 3 - Suite 130
2222 South Dobson Road
Mesa, AZ 85202-6481

AESI
Attn: Bill Todorof
20442 Sun Valley Drive
Laguna Beach, CA 92651

Alabama Power Co.
Attn: Herbert M. Boyd
600 No. 18th Street
Birmingham, AL 35291

American Power Conversion Corp.
Attn: Mr. Ervin F. Lyon
89 Cambridge Street
Burlington, MA 01803-4115

Applied Solar Energy Corp.
Atn: R. F. Brown
15703 E. Valley Blvd.
City of Industry, CA 91749

ARCO Solar Inc.
Attn: Mr. James Caldwell, President
Mr. Elliott Berman
Mr. Charles Helseth
P. O. Box 2105
Chatsworth, CA 91311

Arizona Public Service Co.
Attn: Thomas C. Lepley
P. O. Box 53999, Mail Sta. 3875
Phoenix, AZ 85072-3999

Arizona Solar Energy Commission
Attn: Mr. Paul Huddy
1645 W. Jefferson
Phoenix, AZ 85007

Arizona State University
Attn: Paul Russell
College of Engineering
Tempe, AZ 85287

Atlantic Solar Power, Inc.
Attn: Paul G. Apple
6455 Washington Blvd.
Baltimore, MD 21227

Automatic Power
Attn: Mr. Guy Priestley
P. O. Box 18738
Houston, Texas 77223

Balance of Systems Specialists, Inc.
7745 E. Redfield Road
Scottsdale, AZ 85260

Battelle Columbus Laboratories
Attn: Mr. Don Carmichael
505 King Avenue
Columbus, Ohio 43201

Bechtel National, Inc.
Attn: Mr. Walt Stolte
P. O. Box 3965
San Francisco, CA 94119

Beckwith Electric Company
Attn: Robert W. Beckwith
11811 62nd St. N.
Largo, FL 33543

Best Power Technology, Inc.
P. O. Box 280
Necedah, Wisconsin 54646

BDM Corporation
Attn: Mr. George Rhodes
1801 Randolph Road
Albuquerque, NM 87106

Black and Veatch
Attn: Mr. Sheldon Levy
1500 Meadow Lake Pkwy.
P. O. Box 8405
Kansas City, MO 64114

Blue Sky Water Supply
Attn: Mr. Ronald W. Shaw, President
P. O. Box 21359
Billings, MT 59104

Bonneville Power Adm.
Attn: Minje Ghim
P. O. Box 3621
Portland, OR 97208

Sam Bunker
International Programs Div.(IPD)
Nat'l Rural Elec. Cooperative Assoc.
1800 Massachusetts Avenue, NW
Washington, DC 20036

California Energy Commission
Attn: Mike DeAngelis
1516 9th Street
Sacramento, CA 95814

Chronar Corp.
Attn: Pandelis Zelissaropoulos
Marketing Dept.
Box 177
Princeton, NJ 08542

Chronar-TriSolar Corp.
Attn: Mr. Anand Rangarajan
10 De Angelo Drive
Bedford, MA 01730

City of Austin Power & Light
Attn: John Hoffner
P. O. Box 1088
Austin, TX 78767

Cleveland State University
Attn: Peter P. Groumpos
1983 E. 24th Street
Cleveland, OH 44115

Ctr for Engr. and
Environmental Research
Attn: Angel Lopez
College Station
Mayaguez, Puerto Rico 00708

Colorado Mountain College
Attn: Steve McCarney
3000 County Road 114
Glenwood Springs, CO 81601

Dess Solar Company
Attn: Stephen J. Dess
12845 Industrial Park Blvd.
Plymouth, MN 55441

Detroit Edison Co.
Attn: George Murray, UTE
2000 2nd Avenue
Rm. 2134 WCB
Detroit, MI 48226

Electric Power Research Inst.
Attn: John Schaefer
R. Ferraro
P. O. Box 10412
Palo Alto, CA 94303

Electric Research and Mgmnt.
Attn: Mr. W. E. Feero
P. O. Box 165
State College, PA 16804

Evans International
Attn: Lynn Hurlbert
3128 West Clarendon Avenue
Phoenix, AZ 85017

Energy Resources International
Attn: Carole Taylor
Golden Gate Energy Center
1055 Fort Cronkhite
Sausalito, CA 94965

ENTECH, Inc.
Attn: Mr. Mark O'Neill
1015 Royal Lane
DFW Airport, TX 75261

Farwest Corrosion Control
17311 S. Main Street
Gardena, CA 90248

Florida Alternative Energy Corp.
Attn: Henry M. Healey
2155 Jason St.
Merritt Island, FL 32952

Florida Power & Light
Attn: R. S. Allan
P. O. Box 14000
Juno Beach, FL 33408

Florida Power & Light
Attn: Gary L. Michel
P. O. Box 529100
Miami, FL 33152

Florida Solar Energy Center
Attn: Gerald Ventre
300 State Rd. 401
Cape Canaveral, FL 32920

GNB Incorporated
Attn: Christine McCarthy
2010 Cabot Boulevard West
Langhorne, PA 19047

GPL Industries
P. O. Box 306
La Canada, CA 91011

Georgia Power Company
Attn: Mr. Clayton Griffin
P. O. Box 4545
Atlanta, GA 30302

Georgia Power Co.
Attn: Ed Ney
7 Solar Circle
Shenandoah, GA 30265

Grundfos Pumps Corp.
Attn: Mr. John Maxwell
2555 Clovis Ave.
Clovis, CA 93612

Heliopower Inc.
Attn: Thomas R. Siebert
One Centennial Plaza 3F,
Piscataway, NJ 08854

Hughes Aircraft Company
Attn: Mr. George Naff
P. O. Box 9399
Building A1, M/S 4C843
Long Beach, CA 90810

Independent Power Co.
Attn: Mr. Sam Vanderhoff
Box 649
North San Juan, CA 95960

Integrated Power Corporation (2)
Attn: Mr. Kenneth Gerken
Mr. Lee Gordon
7524 Standish Pl.
Rockville, MD 20855

Intersol Power Corporation
Attn: Mr. John Sanders
11901 W. Cedar Avenue
Lakewood, CO 80228

Interstate Solar Coordination Council
Attn: John R. Dunlop
900 American Center Building
St. Paul, MN 55101

Iota Engineering
4700 S. Park Ave. - Suite 8
Tucson, AZ 85714

IT Power, Inc. (2)
Attn: Thomas Hoffman
Bernard NcNelis
Suite 801
1015 Eighteenth St. NW
Washington, DC 20036

Irridelco Corp., Inc.
440 Sylan Avenue
Inglewood Cliff, NJ 07632

Jacuzzi, Inc.
12401 Interstate 30
P.O. Box 8903
Little Rock, AR 72219-8903

Jensen Brothers Manufacturing Co.
14th and Pacific
P. O. Box 477
Coffeyville, KS 67337

William Lamb Company
Attn: Mr. William Lamb
10615 Chandler Blvd.
North Hollywood, CA 91601

March Manufacturing Co.
1819 Pickwick Avenue
Glenview, IL 60025

Marvel
Attn: Mr. Richard Detrick
P. O. Box 997
Richmond, Indiana 47374

Mass PV Center
Attn: Kevin Collins
1 Mass Tech Center
So. Access Road
Logan Airport
East Boston, MA 02128

A. Y. McDonald Mfg. Co.
Attn: Mr. John D. Eckel
Manager - Energy Products
4800 Chavenelle Road
Dubuque, IA 52001

Meridian Corporation
Attn: Judy Laufman
Judith M. Siegel
5113 Leesburg Pike, Suite 700
Falls Church, Virginia 22041

Mobil Solar Energy Corp.
Attn: Mr. Paul Wormser
16 Hickory Drive
Waltham, MA 02254

National Association of
Home Builders
Attn: Dion Howard
15th and M Street NW
Washington, DC 20036

NAHB Research Foundation, Inc.
Attn: Larry Zarker
700 Prince Georges Center Blvd.
Upper Marlboro, MD 20772

Natural Power, Inc.
Attn: Brian Gordon
Francestown Turnpike
New Boston, NH 03070

Naval Civil Engineering Lab
Attn: Kwang Ta Huang
CODE L 72
Port Hueneme, CA 93043

Naval Weapons Center
Attn: G. Smith
Code 02A1
China Lake, CA 93555-6001

New England Power Service
Attn: Mr. Edward Gulachenski
25 Research Drive
Westborough, MA 01581

Omnion Power Engineering
Attn: Mr. Hans Meyer
W297 S11085 Hwy. ES
Mukwonago, WI 53149

Oxi Oxiders Inc.
Attn: Donald E. Meyers
4990 Euclid Road
Virginia Beach, VA 23462

Pacific Gas & Electric Co.
Attn: Steve Hester
3400 Crow Canyon Road
San Ramon, CA 94583

Photocomm, Inc.
Attn: Mr. Joseph Garcia
7735 East Redfield
Scottsdale, AZ 85260

Photovoltaics International
Attn: Mark Fitzgerald
Box 1467
Denver, CO 80201

PV Energy Systems, Inc.
Attn: Mr. Paul Maycock
P. O. Box 290
Casanova, VA 22017

Platte River Power Authority
Attn: Carol J. Dollard
Timberline & Horsetooth Roads
Fort Collins, CO 80525

Polar Products
Attn: Mr. Arthur Sams
2908 Oregon Court
Building I-11
Torrance, CA 90503

Public Service Co. of New Mexico
Attn: Mr. R. Michael Lechner
Alvarado Square
Albuquerque, NM 87158

Public Service Elec. & Gas. Co.
Attn: Mr. Harry Roman
80 Park Plaza
P. O. Box 80
Newark, NJ 07101

Pulstar
619 South Main St.
Gainesville, FL 32601

Renewable Energy Institute
Attn: Robert Hayden
1516 King Street
Alexandria, VA 22314

Research Triangle Institute
Attn: Carl Parker
P. O. Box 12194
Research Triangle Park, NC 27709

Robbins and Myers
P. O. Box 965
Springfield, OH 45501

Miles C. Russell
11 Forest Glen Road
Reading, MA 01867

Salt River Project
Attn: Mr. Steve Chalmers
P. O. Box 1980
Phoenix, AZ 85001

San Diego Gas & Electric
Attn: Don E. Fralick
P. O. Box 1831
San Diego, CA 92112

Simpler Solar Systems
3120 W. Thorpe
Tallahassee, FL 32302

Six Rivers Solar, Inc.
Attn: Greg Williams
818 Broadway
Eureka, CA 95501

Solar Economics, Inc.
Attn: Martin Katzman
7271 Dye Drive
Dallas, TX 75248

Solar Electric Engineering
Attn: Hugh Diaz
405 East "D" St.
Petaluma, CA 94952

Solar Electric Specialties
Attn: Jim Welch
1558 Riverside
Fort Collins, CO 80524

Solar Electric Systems
Attn: Richard V. Collins
4747 Troost Avenue
Kansas City, MO 64110

Solar Energy Industries Assn. (2)
Attn: David Gorin
Scott Sklar
1720 N. Lynn St.
Arlington, VA 22209-2009

Solar Energy Research Inst. (5)
Attn: Richard DeBlasio
Donna Hawkins
Bob McConnell
Tom Surek
Ed Witt
1617 Cole Blvd.
Golden, CO 80401

Solar Engineering Services
Attn: Mr. Tim Ball
P. O. Box 7122
Olympia, WA 98507

Solar Trade International
Attn: Manuel J. Blanco
630-6th Avenue - Suite 2M
San Francisco, CA 94118

Solar Works
Attn: Leigh Seddar
13 Bailey Ave.
Montpelier, VT 05602

Solarex Corporation (2)
Attn: Mr. Malcolm L. Ream
Mr. Ted Blumenstock
1335 Piccard Drive
Rockville, MD 20850

Solavolt International
Attn: Mr. Paul Garvison
P. O. Box 2934
Phoenix, AZ 85062

Solec International, Inc.
Attn: Ishaq Shahryar
12533 Chadron Avenue
Hawthorne, CA 90250

Southern California Edison
Attn: Mr. Nick Patapoff
P. O. Box 800
Rosemead, CA 91770

Southern Company Services
Attn: Mr. J. Timothy Petty
P. O. Box 2625
Birmingham, AL 35202

Specialty Concepts, Inc.
9025 Eton Ave., Suite D
Canoga Park, CA 91304

Spire Corporation
Attn: Mr. Roger Little
Patriots Park
Bedford, MA 01730

Stone & Webster Engr. Corp.
Attn: Mr. Duncan Moodie
245 Summer St.
Boston, MA 01921

Strategies Unlimited (2)
Attn: Mr. Bill Murray
Mr. Robert Steele
201 San Antonio Circle
Suite 205
Mountain View, CA 94040

SW RES Experiment Station
Attn: Vern Risser
New Mexico State University
Box 3SOL
Las Cruces, NM 88003

Tennessee Valley Authority (2)
Attn: Joan Wood
Sharon Ogle
Solar Applications Branch
350 Credit Union Building
Chattanooga, TN 37401

Tideland Signal Corp.
Attn: Mr. Harry Saenger
4310 Director's Row
P. O. Box 52430
Houston, TX 77052

University of Lowell
Attn: Jose Martin
Mechanical Engineering Dept.
Lowell, MA 01854

University of Lowell (2)
Attn: Thomas Costello
Fahd Wakim
1 University Avenue
Lowell, MA 01854

University of Texas
at Arlington
Attn: Jack Fitzer
West 6th at Speer Street
Arlington, TX 76019

U.S. Agency for International
Development (USAID)
Attn: Mr. Jack Vanderryn
Director, Energy and Natural
Resources
Rm. 509, SA-18
Washington, DC 20523

U.S. Department of Energy (3)
PV Energy Technology Division
Attn: Mr. R. H. Annan
Mr. A. Krantz
Mr. V. Rice
1000 Independence Avenue SW
Washington, DC 20585

U.S. Dept. of Energy (2)
Attn: Dean Graves
Joe Weisiger
Energy Technology Division
Albuquerque Operations Office
Albuquerque, NM 87115

U.S. Department of Energy
Attn: Leonard J. Rogers
Wind/Ocean Technologies Div.
1000 Independence Ave. SW
Washington, DC 20585

U.S. Department of Energy
Attn: J. Rumbaugh
DOE/Wind Systems
1000 Independence Ave., SW
Washington, DC 20585

U.S. Virgin Islands Energy Office
Institutional Conservation Program
Lagoon Complex, Bldg. 3, Room 233
St. Croix, U.S. Virgin Islands 00840

Warns Solar Pumps
Attn: Mr. Robert Meyer
246 East Irving
Wood Dale, IL 60191

Westinghouse Advanced Energy
Systems Division (2)
Attn: J. Robert Maxwell
Marketing Manager
P. O. Box 158
Madison, PA 15663

The World Bank
Attn: Walter Vergara
Industry Department
1818 H Street, N.W.
Washington, DC 20433

Zomeworks
Attn: Steve Baer
P. O. Box 25805
Albuquerque, NM 87125

6200 V. L. Dugan
6220 D. G. Schueler
6223 G. J. Jones
6223 W. I. Bower
6223 R. N. Chapman (100)
6223 T. S. Key
6223 D. F. Menicucci
6223 H. N. Post
6223 J. W. Stevens
6223 M. G. Thomas
3141 J. A. Landenberger (5)
3151 W. L. Garner (3)
3154-1 C. H. Dalin (28) for DOE/OSTI
8024 P. W. Dean